LASER REMOTE SENSING

PART I

Eduardo Landulfo

elandulf@ipen.br

https://www.youtube.com/watch?v=SaBLaLnRm24

SOME HISTORY…

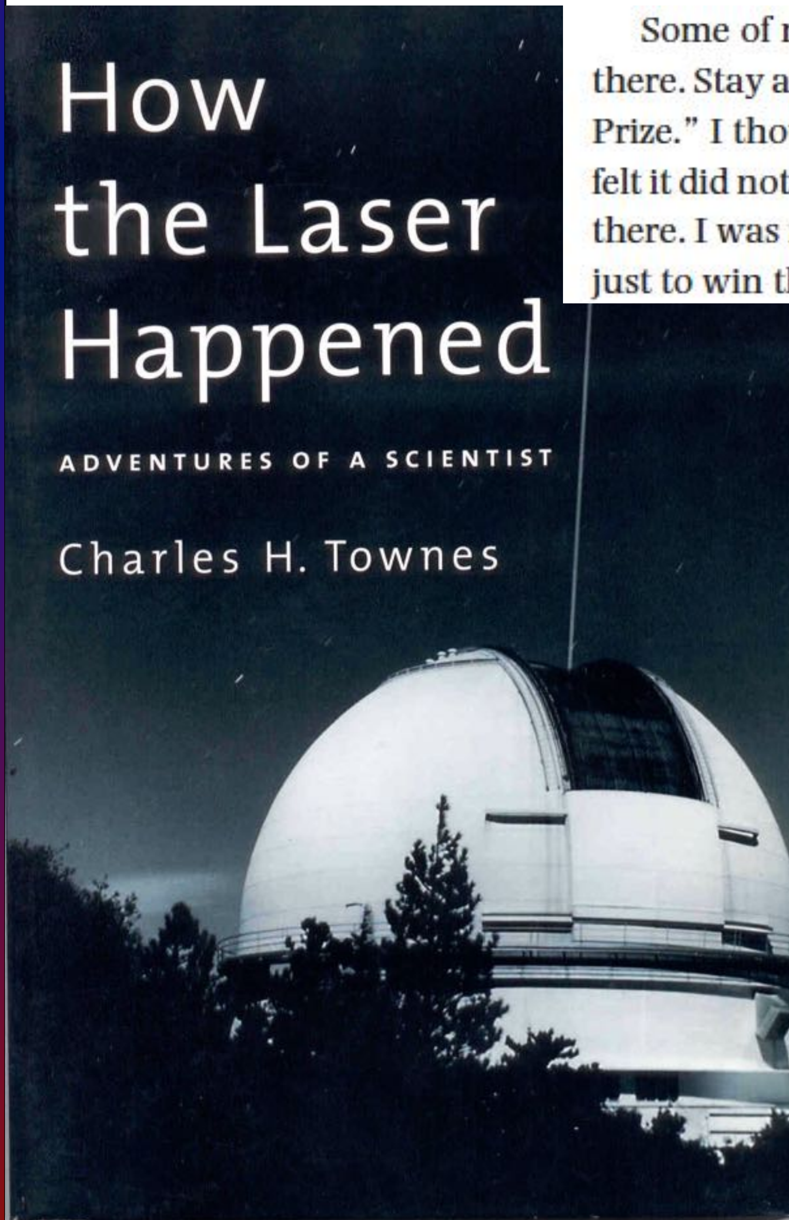

Some of my colleagues warned me in various ways, "Don't go down there. Stay and build the laser. That is the work that will get you the Nobel Prize." I thought the maser and laser might, in fact, win a Nobel. But, I felt it did not really matter who actually built the first one. The ideas were there. I was not going to make a career decision to go all-out to build one just to win the prize.

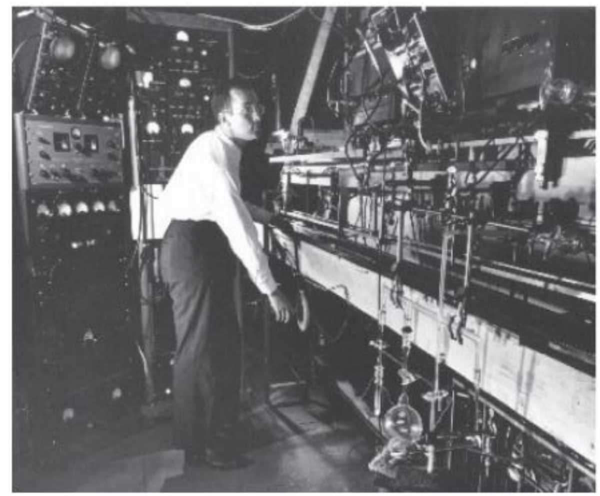

Figure 7. My apparatus for measuring microwave spectra of molecules, built with my students at Columbia University, 1949.

SOME HISTORY...

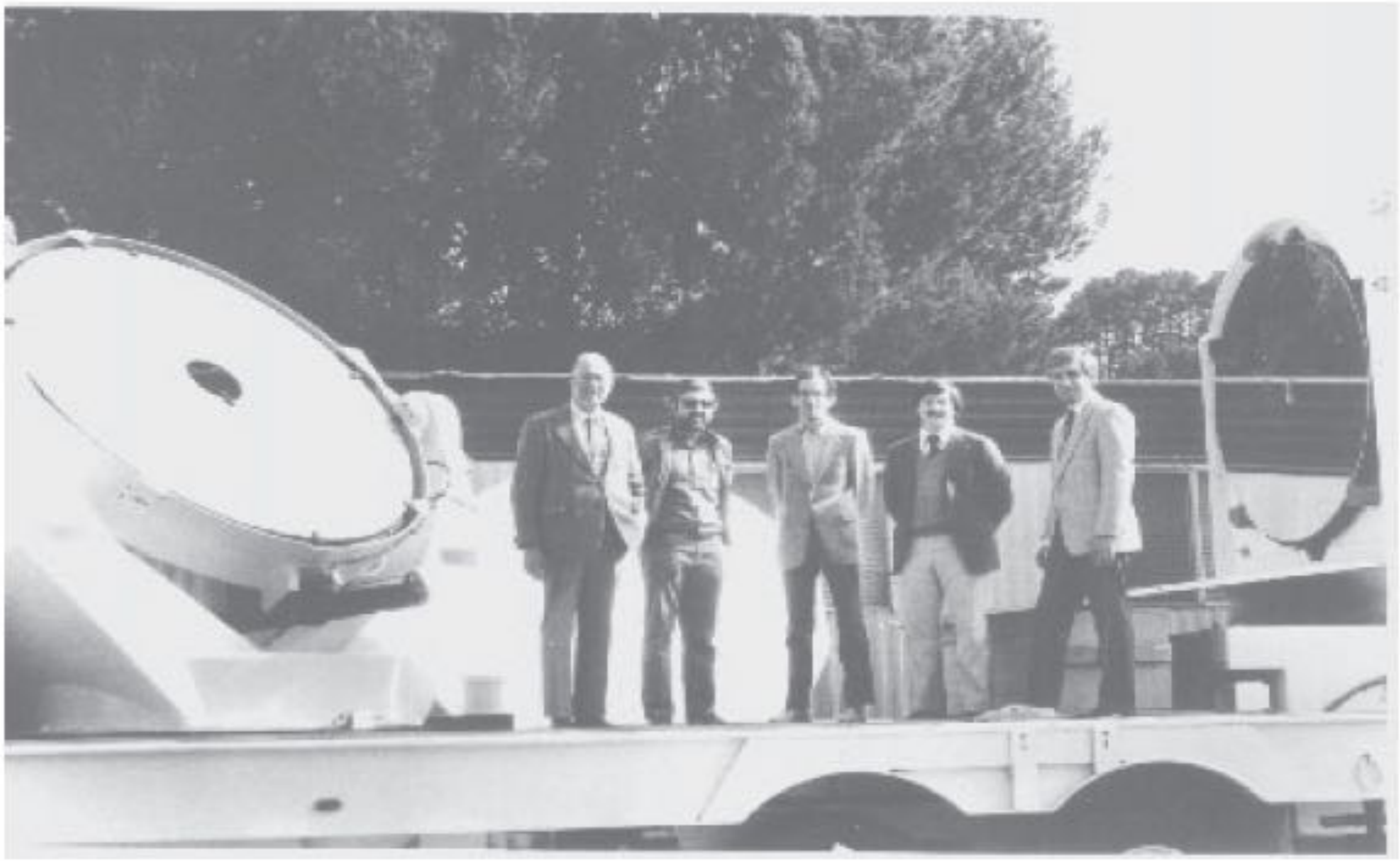

Figure 16. The christening at the University of California of our first large movable telescope on a trailer, one unit of the Infrared Spatial Interferometer, which maps the details of stellar shapes and the clouds around stars. In operation, laser beams shine back and forth between the two mirrors. Left to right are Charles Townes, electronics technician Walter Fitelson, and physicists Edmund Sutton, William Danchi, and Manfred Bester.

TWO BASIC QUESTIONS:

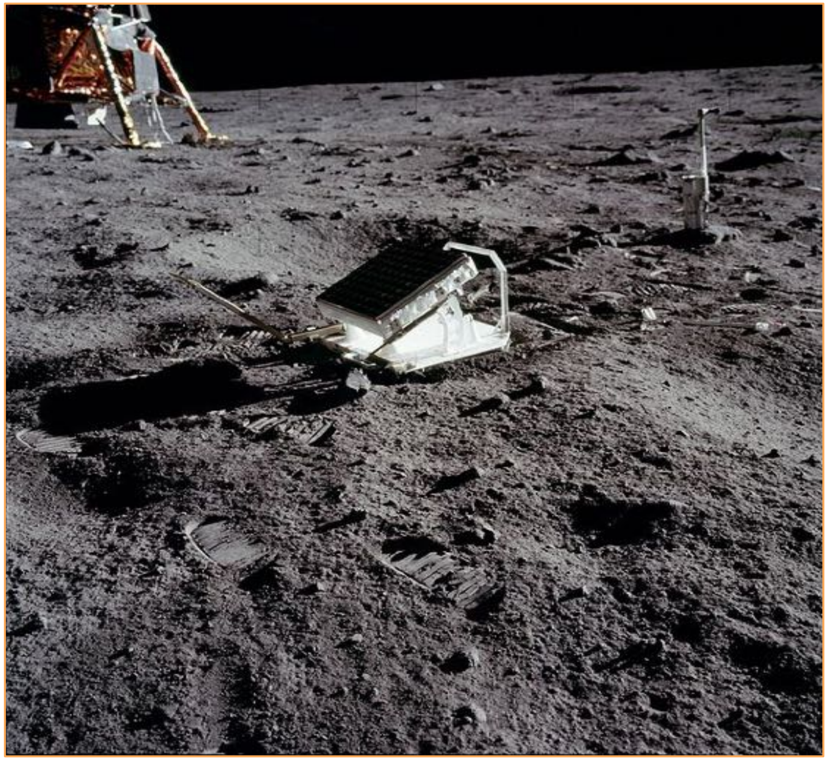

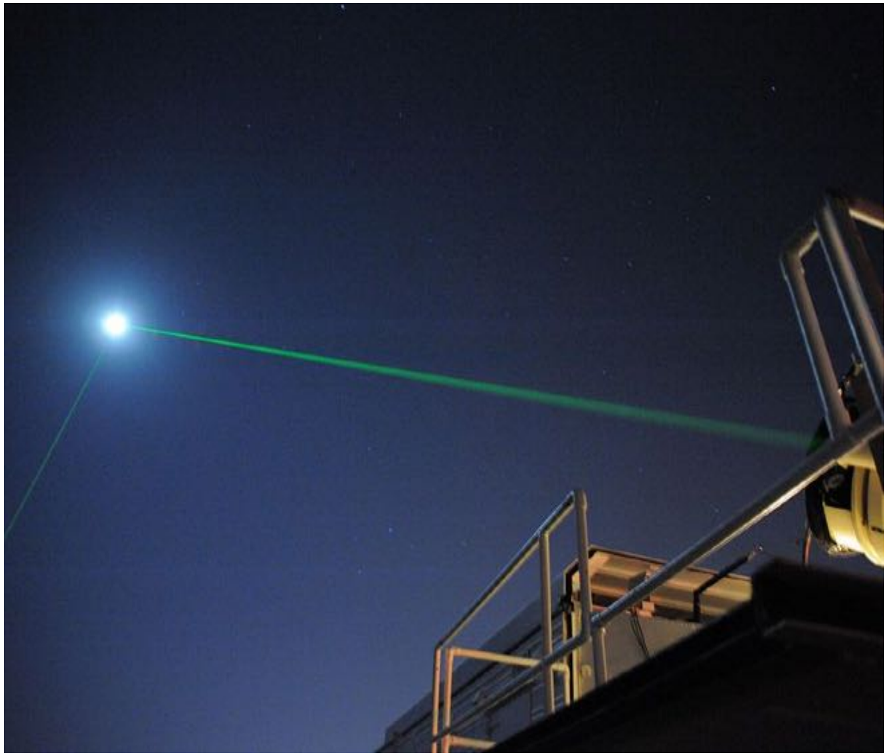

WHAT'S THE DISTANCE BETWEEN THE MOON AND THE EARTH?

HOW MUCH "MATTER" IS BETWEEN THE TWO ?

NON-COHERENT APPROACHES

1930 Synge proposed a method to determine the atmospheric density with an anti-aircraft searchlight and a telescope (bistatic configuration)

1936 First reported results of density profiles: **Duclaux** (3.4 km), **Hulbert** (28 km)

1938 First reported use of **a monostatic configuration for cloud base height, using a pulsed light source (**Bureau)

1953 First retrieval of temperature profiles from density profiles (**Elterman**)

HOMEWORK: TRY DOING AT HOME...

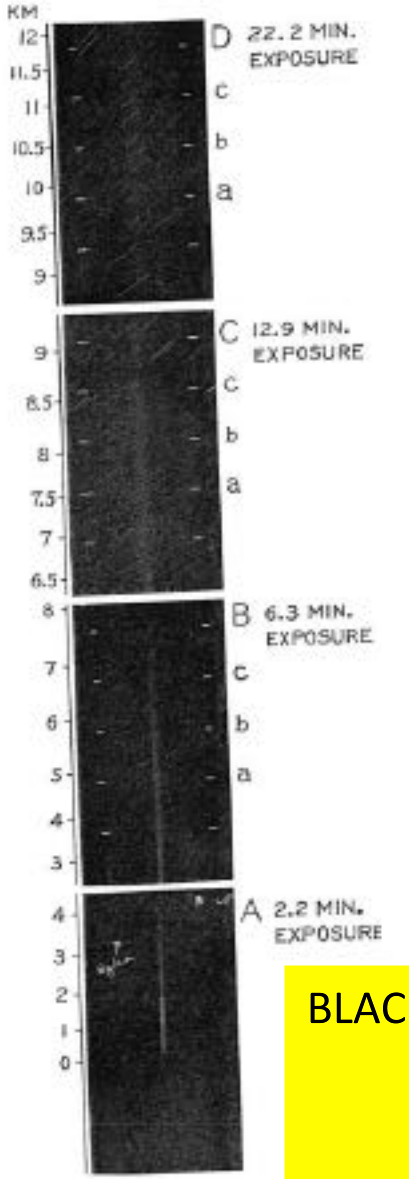

FIG. 1. Photographs of sear

It is difficult to estimate the possible errors in the numbers of columns (3) and (4), Table I; they, and those of column (5), may be correct within a factor of 2. With this qualification the theoretical intensities of column (4) deviate in a regular manner from the observed intensities of column (3) as shown by the ratios of column (5). The ratios decrease from about 7 at 5 km to unity at 10 or 15 km. The deviations would be

[5] Humphreys, *Physics of the Air* (1929), p. 74.

APPENDIX 1

Photographic determination of the intensity of the beam

A ribbon filament tungsten lamp, standardized by the National Bureau of Standards, burning at a red ($\lambda 0.655\mu$) black body apparent temperature of 1719°K, served as a known source of energy. A diaphragm limited the exposed area of the filament to 0.124 cm². A selected blue filter of known transmission was placed in front of the lamp; the spectral energy curve of the light through the filter is given in curve 1, Fig. 3. The calculated spectral energy curve of the scattered light of the searchlight beam is

TABLE II. *Average temperature and density of the atmosphere.*

ALTITUDE	TEMP.	DENSITY d	n	ALTITUDE	TEMP.	DENSITY d	n
0 km	1.72°C	1256×10^{-6}	261×10^{17}	20 km	−55°C	89.7×10^{-6}	18.6×10^{17}
2	−4.16	1010	210	22	−55	65.8	13.7
4	−15.3	817	170	24	−55	48.2	10.0
6	−29.3	660	137	26	−55	35.3	7.32
8	−43.6	529	110	28	−55	25.9	5.39
10	−54.2	414	86.0	30	−55	19.0	3.95
12	−55	311	64.5	32	−55	13.9	2.89
14	−55	228	47.5	34	−55	10.2	2.12
16	−55	167	34.7	36	−55	7.54	1.57
18	−55	121	25.2	38	−55	5.53	1.15

BLACK BODY AT 1719 K

BLUE FILTER

655 nm

Inverse square law

$$\frac{d\sigma_e}{d\Omega} = \frac{8\pi}{3}.\frac{\pi^2(n^2-1)^2}{N^2\lambda^4}(cos^2\theta cos^2\phi + sen^2\theta)$$

RAYLEIGH SCATTERING

ALMOST 30 YEARS LATER...

LIght Detection And Ranging

551.501.71 : 551.508.93 : 538.8

Lidar : a new atmospheric probe

By R. T. H. COLLIS
Stanford Research Institute, Menlo Park, California

(Manuscript received 26 July 1965; in revised form 6 December 1965)

SUMMARY

Pulsed-light techniques of probing the atmosphere have been greatly extended by employing lasers as energy sources in instruments called ' lidars.' Because of the nature of laser energy and the manner in which it is used in current and proposed systems, lidar is best discussed in terms of radar. Apart from the basic capabilities of lidar for detecting backscattering from atmospheric constituents, possibilities exist for more sophisticated techniques based on the wave nature of the energy. The basic capabilities of lidar, however, make it possible to observe the atmosphere with previously unknown resolution and sensitivity. Apart from providing new information about clouds, lidar has shown that the concentration of the particulate matter content of clear air is highly variable and that such variations can indicate the structure and motion of the clear atmosphere. These capabilities have applications in atmospheric and meteorological research and various operational activities.

PERHAPS THE FIRST TIME THE WORD (ACRONYM) LIDAR *was used*

LIDAR : A NEW ATMOSPHERIC PROBE 223

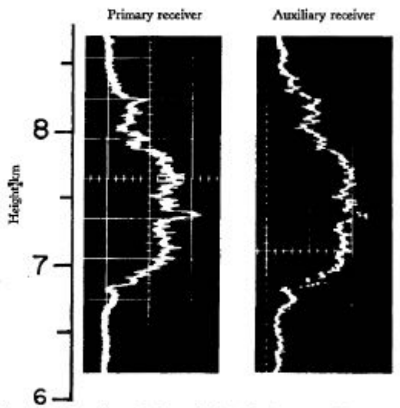

Figure 1. Simultaneous observations of cirrus cloud 4 October 1965. The two traces show the returns (relative intensity vs height) from cirrus cloud as observed simultaneously by the SRI Mark II 1965 lidar and an auxiliary receiver located at a distance of 17 m.

R.T. H. Collins, Lidar: A new atmospheric probe, Quart. J. Royal Meteor. Society, 220-230, 1966

ATMOSPHERIC WINDOW

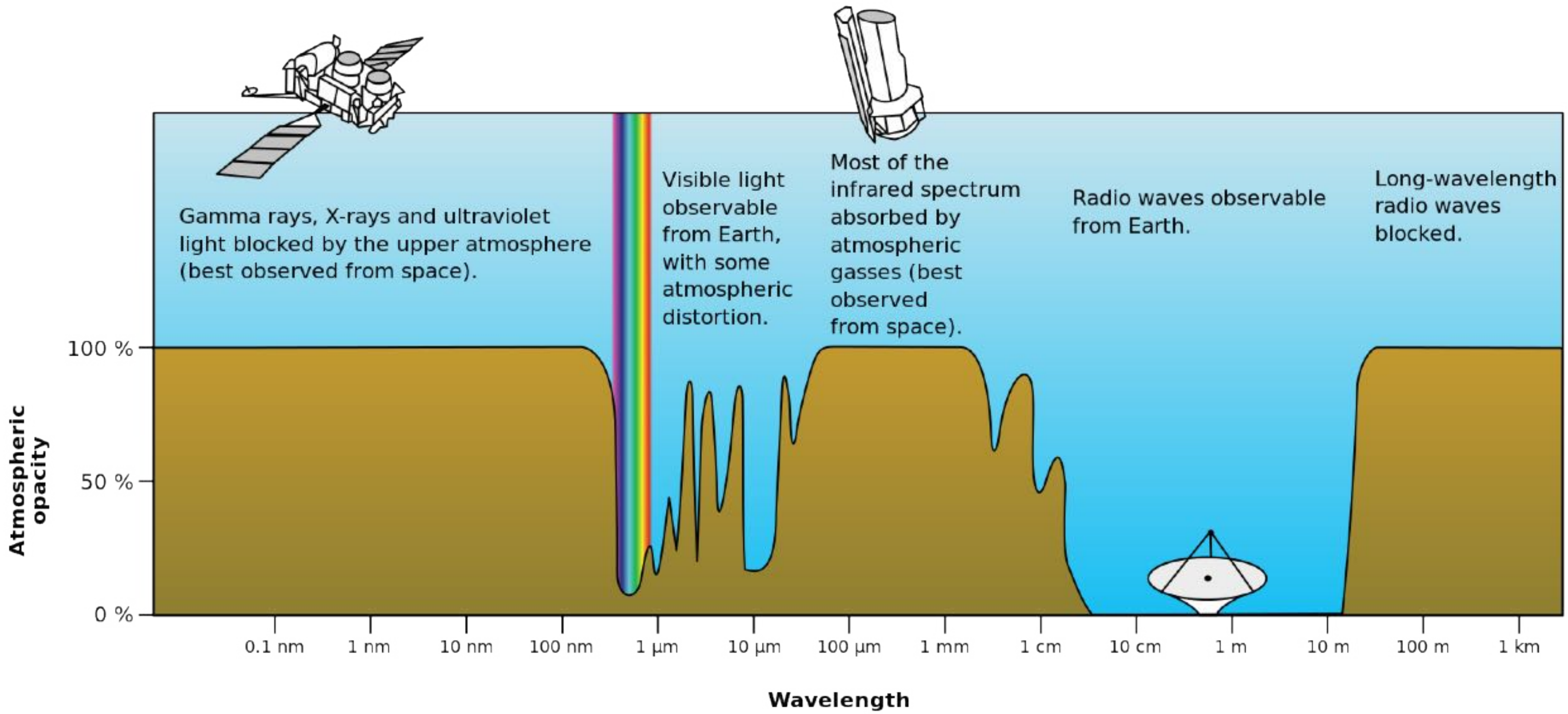

ATMOSPHERIC WINDOW

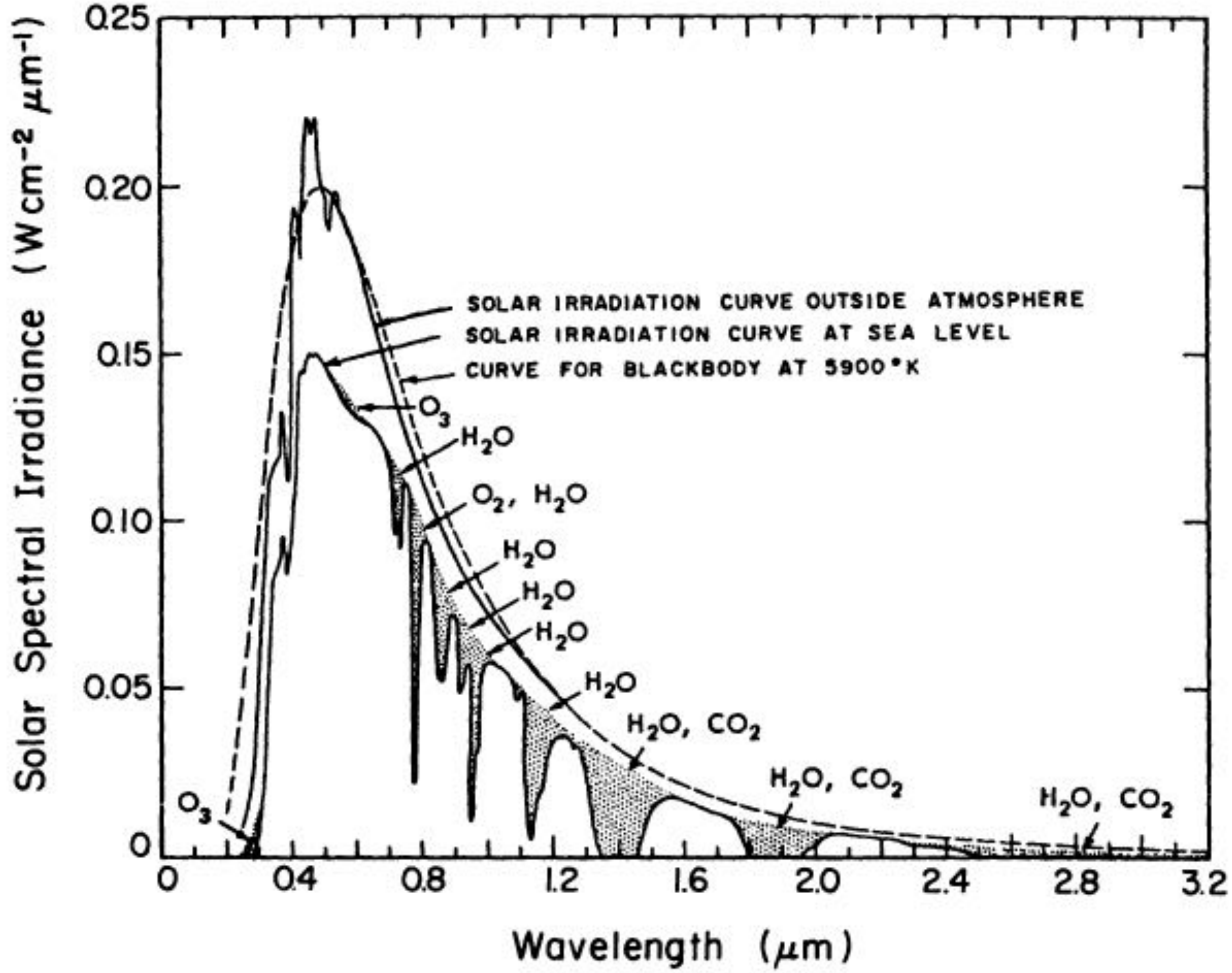

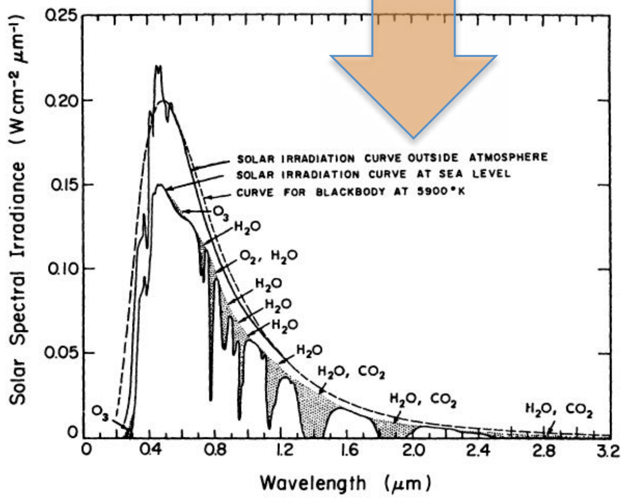
Solar Spectral Irradiance (W cm⁻² µm⁻¹)
Wavelength (µm)
SOLAR IRRADIATION CURVE OUTSIDE ATMOSPHERE
SOLAR IRRADIATION CURVE AT SEA LEVEL
CURVE FOR BLACKBODY AT 5900°K
O3
H2O
O2, H2O
H2O, CO2
0.25
0.20
0.15
0.10
0.05
0
0.4
0.8
1.2
1.6
2.0
2.4
2.8
3.2

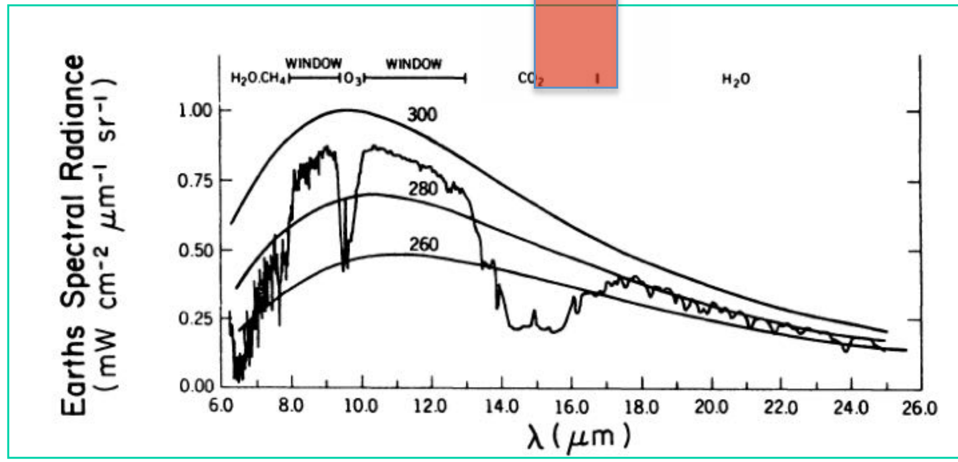
Earths Spectral Radiance
(mW cm⁻² µm⁻¹ sr⁻¹)
λ (µm)
WINDOW
WINDOW
H2O.CH4
O3
CO2
H2O
300
280
260
1.00
0.75
0.50
0.25
0.00
6.0
8.0
10.0
12.0
14.0
16.0
18.0
20.0
22.0
24.0
26.0

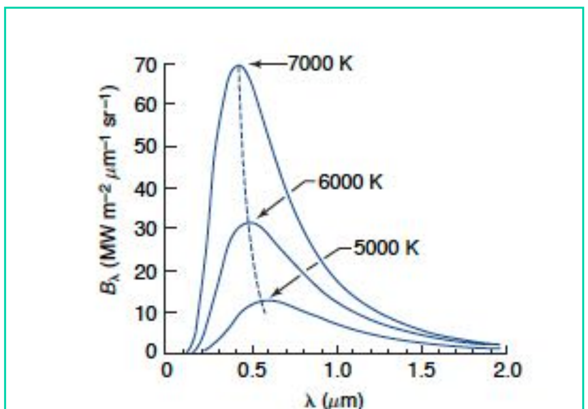
Bλ (MW m⁻² µm⁻¹ sr⁻¹)
λ (µm)
7000 K
6000 K
5000 K
70
60
50
40
30
20
10
0
0.5
1.0
1.5
2.0

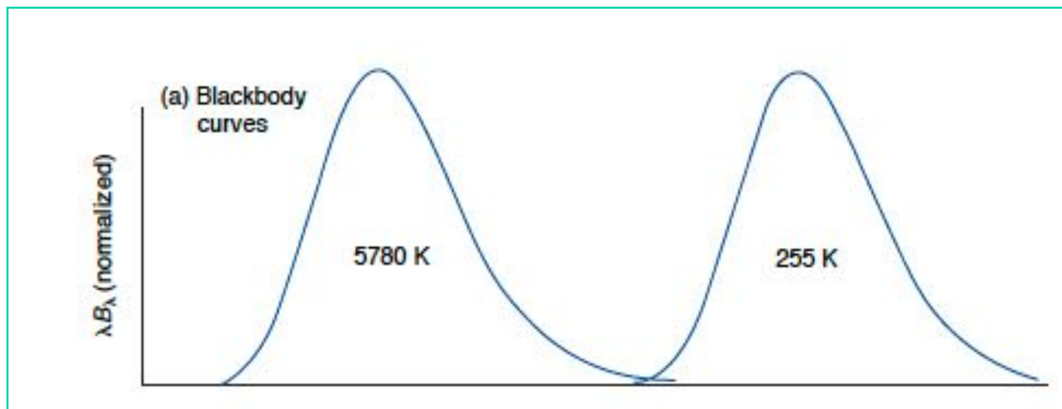
(a) Blackbody curves
λBλ (normalized)
5780 K
255 K

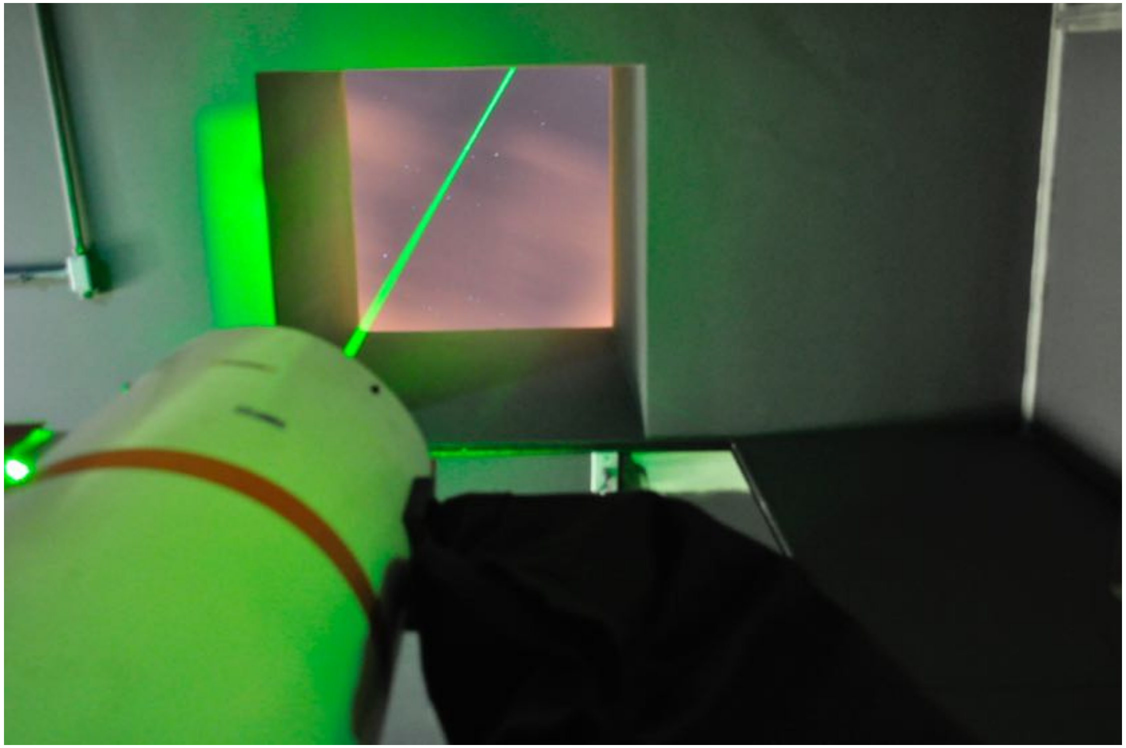

WHAT HAPPENS WHEN ONE SENDS A LASER BEAM INTO THE ATMOSPHERE ?

THE SCATTERING MECHANISMS…

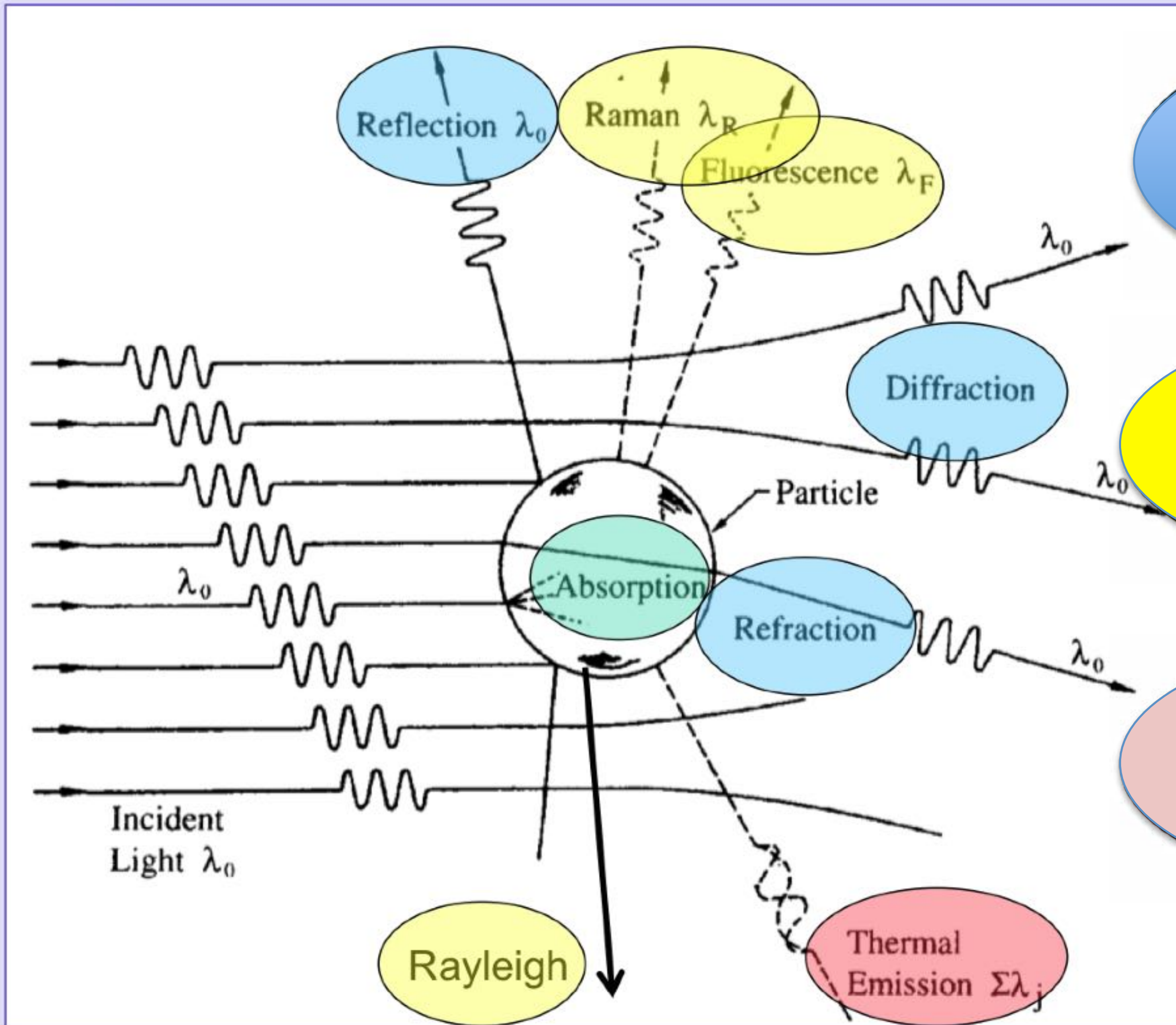

GEOMETRICAL OPTICS

QUANTUM MECHANICS

THERMODYNAMICS

PLANET EARTH IS BLUE AND THERE IS NOTHING WE CAN DO BUT…

Scattering type	Cross section (cm^2)	Ratio (%)
Rayleigh	1.156×10^{-27}	100
O_2 RRS	7.10×10^{-29}	6.1
N_2 RRS	2.94×10^{-29}	2.5
Air RRS	3.82×10^{-29}	3.3
VRS	–	0.1

RAYLEIGH SCATTERING – INTENSITY

The Intensity of the scattered light is proportional to the inverse of the fourth power of the EM wavelength.

$$I_\lambda \sim 1/\lambda^4.$$

BLUE *vs* GREEN

$$\frac{\lambda_1}{\lambda_2} = (440\,/\,550)^4$$

$$\frac{256}{625}$$

% // N

0.4096

A LITTLE BIT OF DIMENSIONAL ANALISYS

$$E_s \propto \frac{E_i V}{r.k}$$

$$[k] = \frac{[E_i][V]}{[r][E_s]}$$

$$[k] = [L]^2 \quad \Rightarrow \quad k = [\lambda]^2$$

A LITTLE BIT MORE OF DIMENSIONAL ANALISYS

RAYLEIGH SCATTERING – DIMENSION ANALYSIS

SCATTERED INTENSITY (POWER)

$$I_s \propto E_s^2$$

$$I_s \propto \frac{E_i^2 V^2}{r^2 \lambda^4}$$

WHY DON'T WE SEE THE SKY AS VIOLET THEN ?

" The wonders of Photoshop and Gimp "

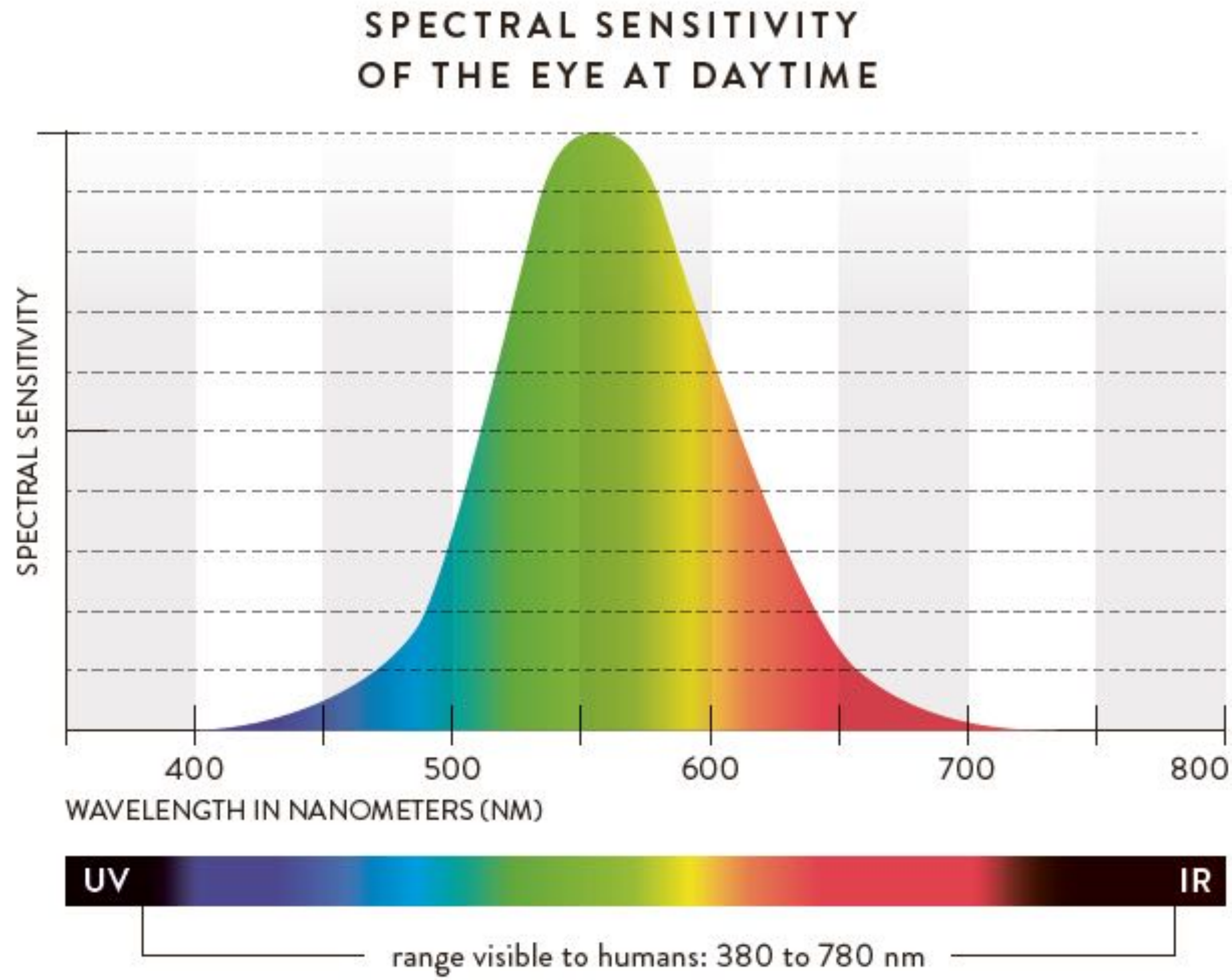
SPECTRAL SENSITIVITY
OF THE EYE AT DAYTIME
SPECTRAL SENSITIVITY
400
500
600
700
800
WAVELENGTH IN NANOMETERS (NM)
UV
IR
range visible to humans: 380 to 780 nm
SPSAS on Atmospheric Aerosols

RAYLEIGH SCATTERING CROSS SECTION

$$\sigma_s = \frac{8\pi^3(m_r^2 - 1)^2}{3\lambda^4 N_s^2}\left(\frac{6+3\delta_p}{6-7\delta_p}\right)$$

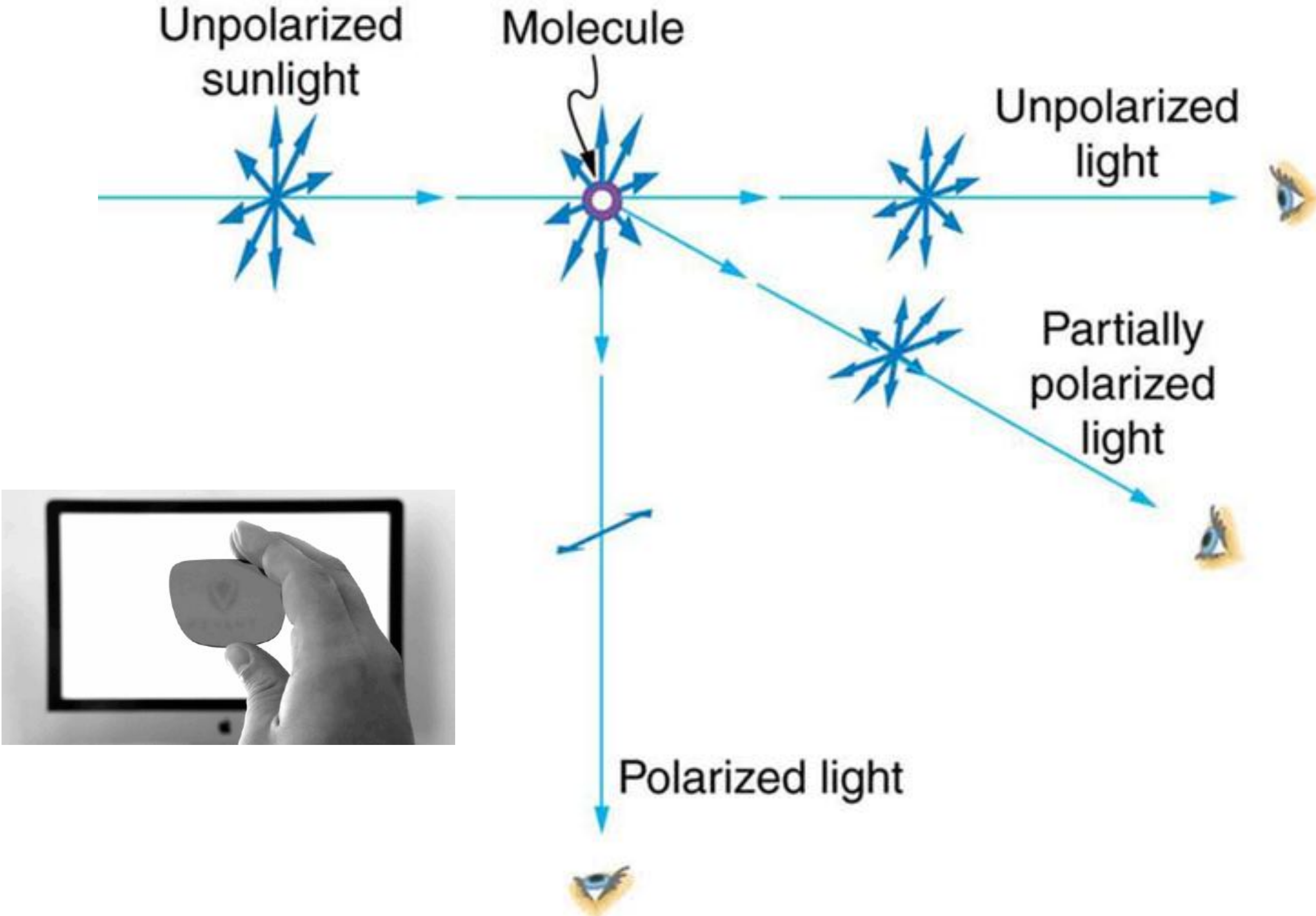
Unpolarized sunlight
Molecule
Unpolarized light
Partially polarized light
Polarized light

IN SEARCH OF ACCURACY

Here we suggest a method for calculation of Rayleigh optical depth that goes back to first principles as suggested by Penndorf (1957) rather than using curve-fitting techniques, although it is true that the refractive index of air is still derived from a curve fit to experimental data. We suggest using all of the latest values of the physical constants of nature, and we suggest including the variability in refractive index, and also the mean molecular weight of air, due to CO_2 even though these effects are in the range of 0.1%–0.01%. It should be noted that aerosol optical depths are often as low as 0.01 at Mauna Loa. Since Rayleigh optical depth is of the order of 1 at 300 nm, it is seen that a 0.1% error in Rayleigh optical depth translates into a 10% error in aerosol optical depth. Furthermore, it simply makes sense to perform the calculations as accurately as possible.

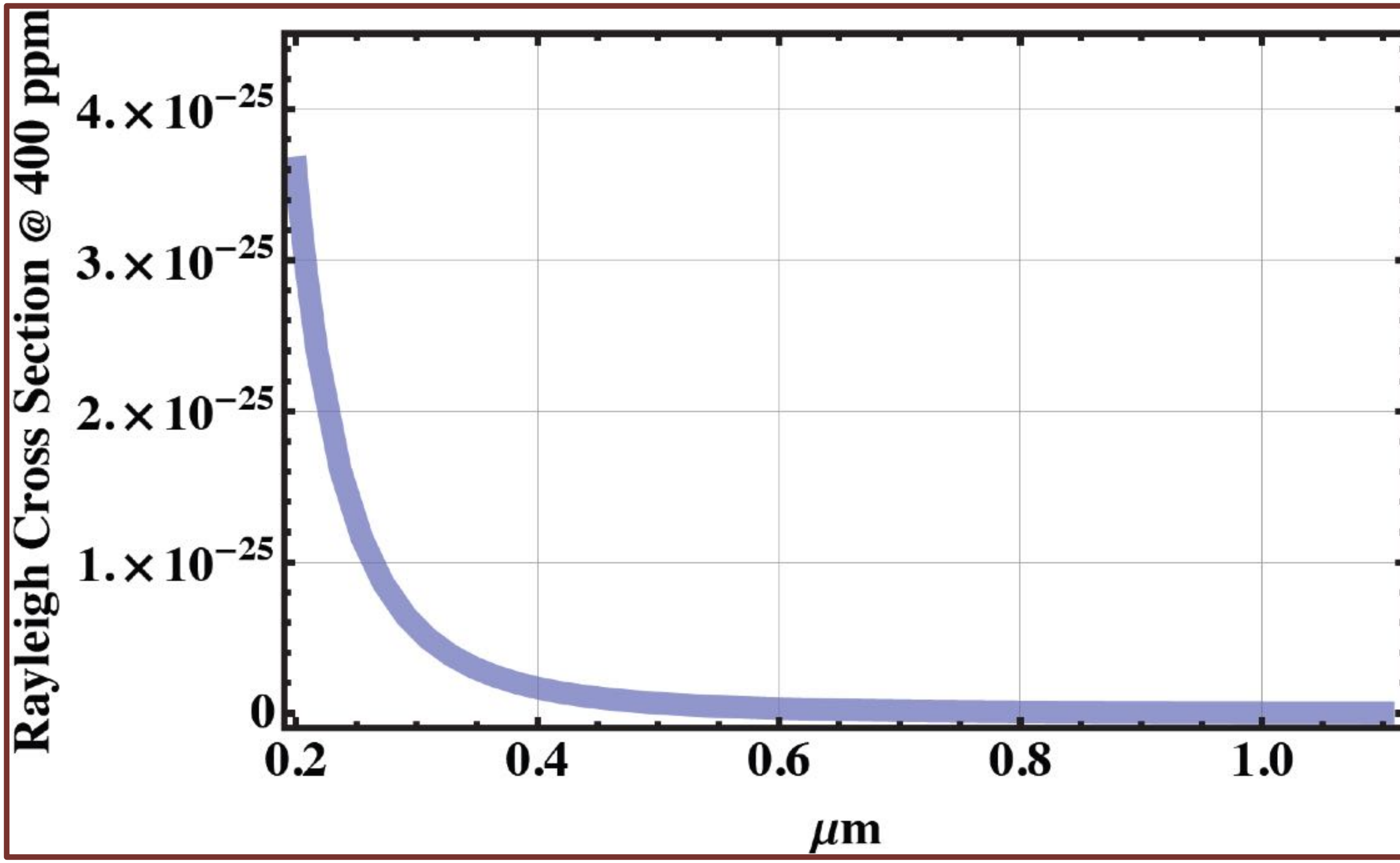
Rayleigh Cross Section @ 400 ppm
4.×10^−25
3.×10^−25
2.×10^−25
1.×10^−25
0
0.2
0.4
0.6
0.8
1.0
μm

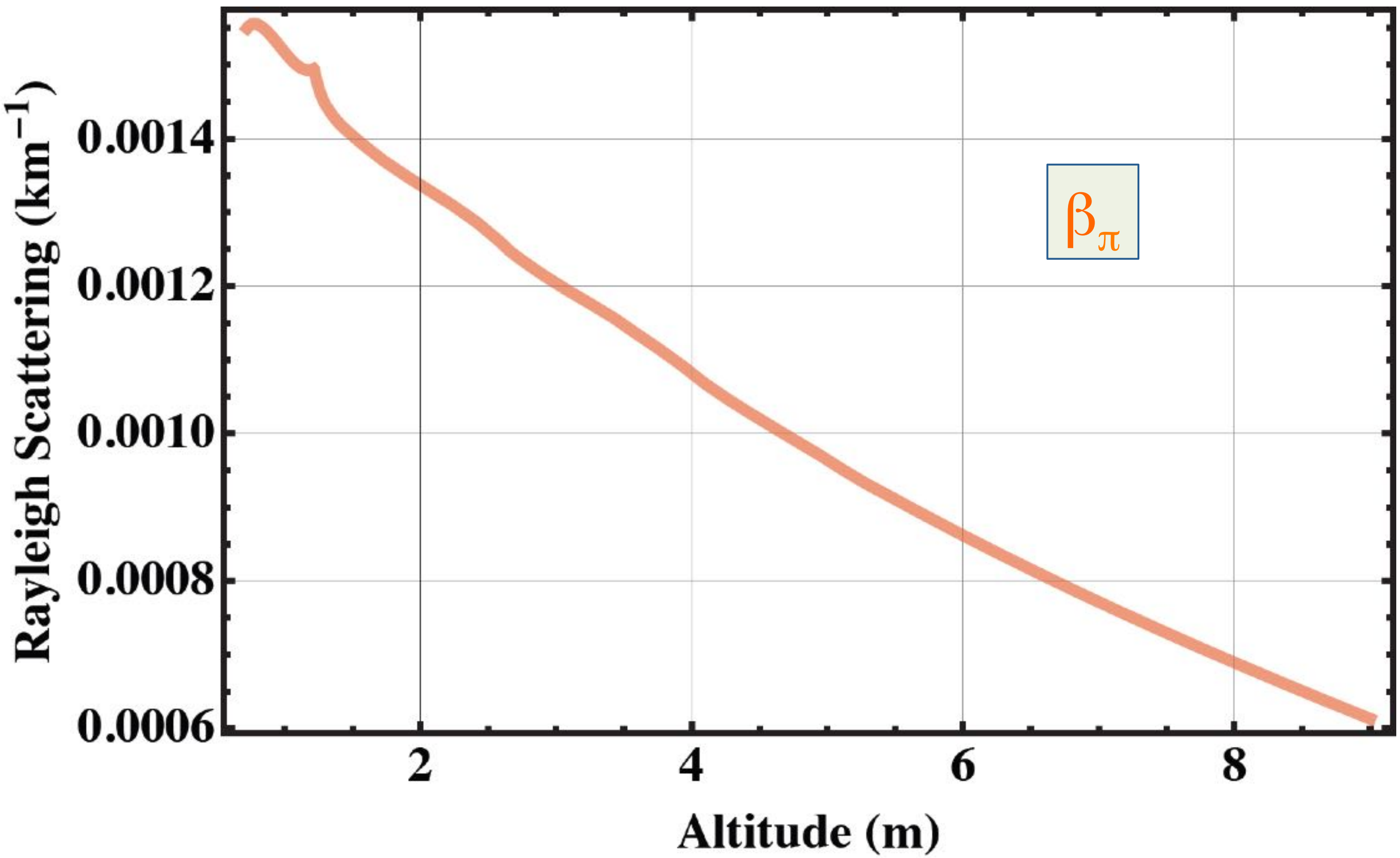
Rayleigh Scattering (km^{-1})
0.0014
0.0012
0.0010
0.0008
0.0006
2
4
6
8
Altitude (m)
β_π

MIE SCATTERING – TOWARDS A BIGGER SCATTERER

RAYLEIGH → MIE

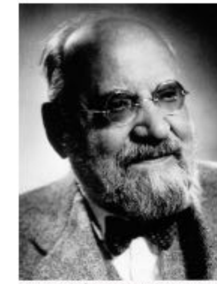

Gustav Mie (29.09.1868 - 13.02.1957)
Professor in Halle 1917-1924

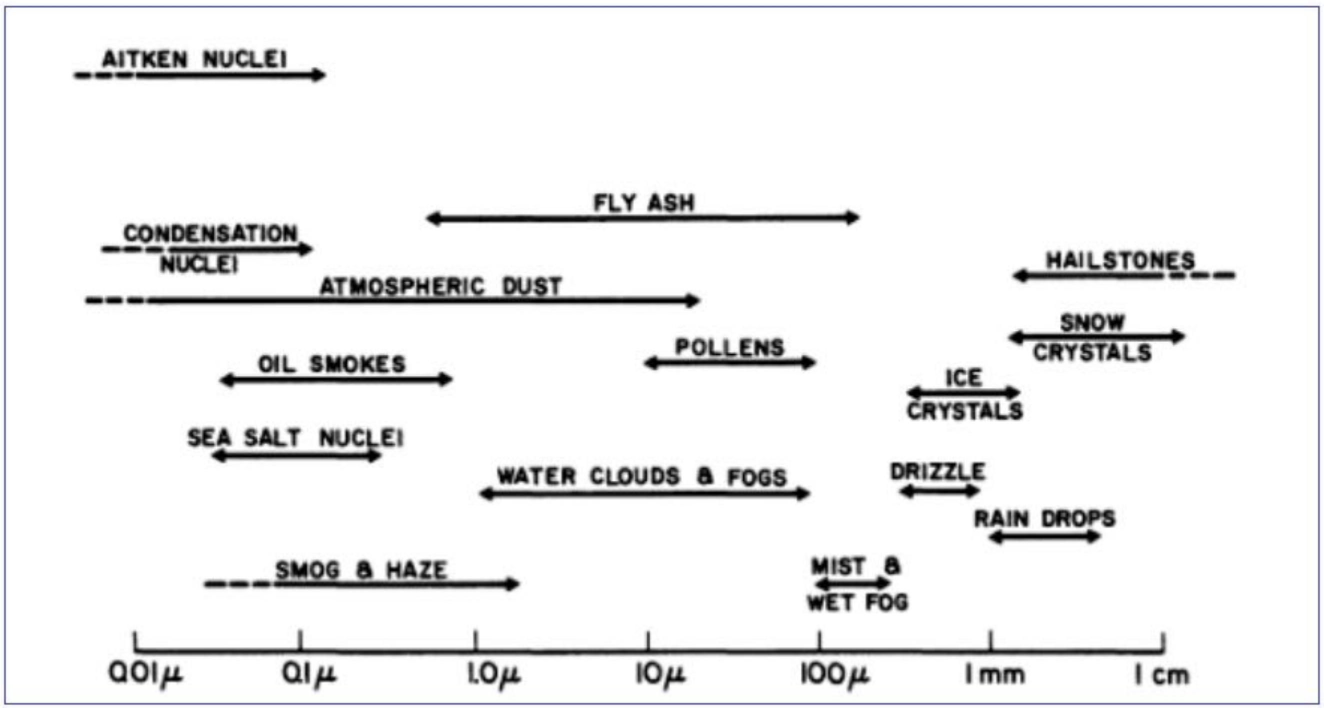

MIE SCATTERING - BUILDING CONCEPTS

SIZE PARAMETER

$$x = \frac{2\pi a}{\lambda}$$

SCATTERING EFFICIENCY

$$Q_s = \frac{\sigma_s}{\pi . a^2}$$

BOTH ADIMENSIONAL QUANTITIES

MIE SCATTERING – TOWARDS A BIGGER SCATTERER

$$x \ll 1$$

RAYLEIGH SCATTERING

$$x \gtrsim 1$$

MIE SCATTERING

Mie Scattering

The scattering from molecules and very tiny particles (< 1 /10 wavelength) is predominantly Rayleigh scattering. For particle sizes larger than a wavelength, Mie scattering predominates. This scattering produces a pattern like an antenna lobe, with a sharper and more intense forward lobe for larger particles.

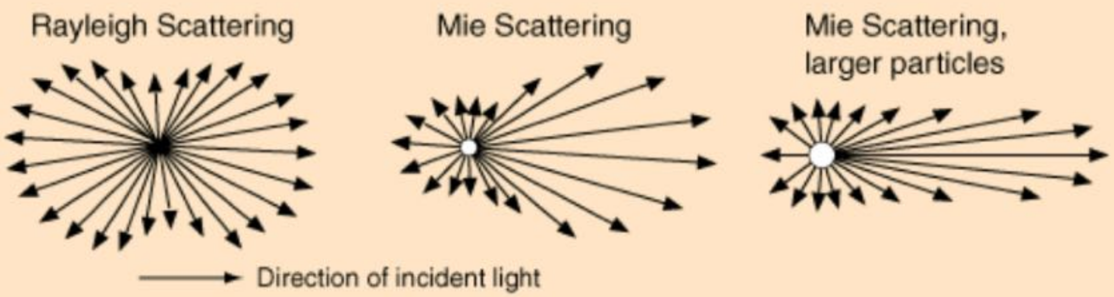

Mie scattering is not strongly wavelength dependent and produces the almost white glare around the sun when a lot of particulate material is present in the air. It also gives us the the white light from mist and fog.

Greenler in his "Rainbows, Haloes and Glories" has some excellent color plates demonstrating Mie scattering and its dramatic absence in the particle-free air of the polar regions.

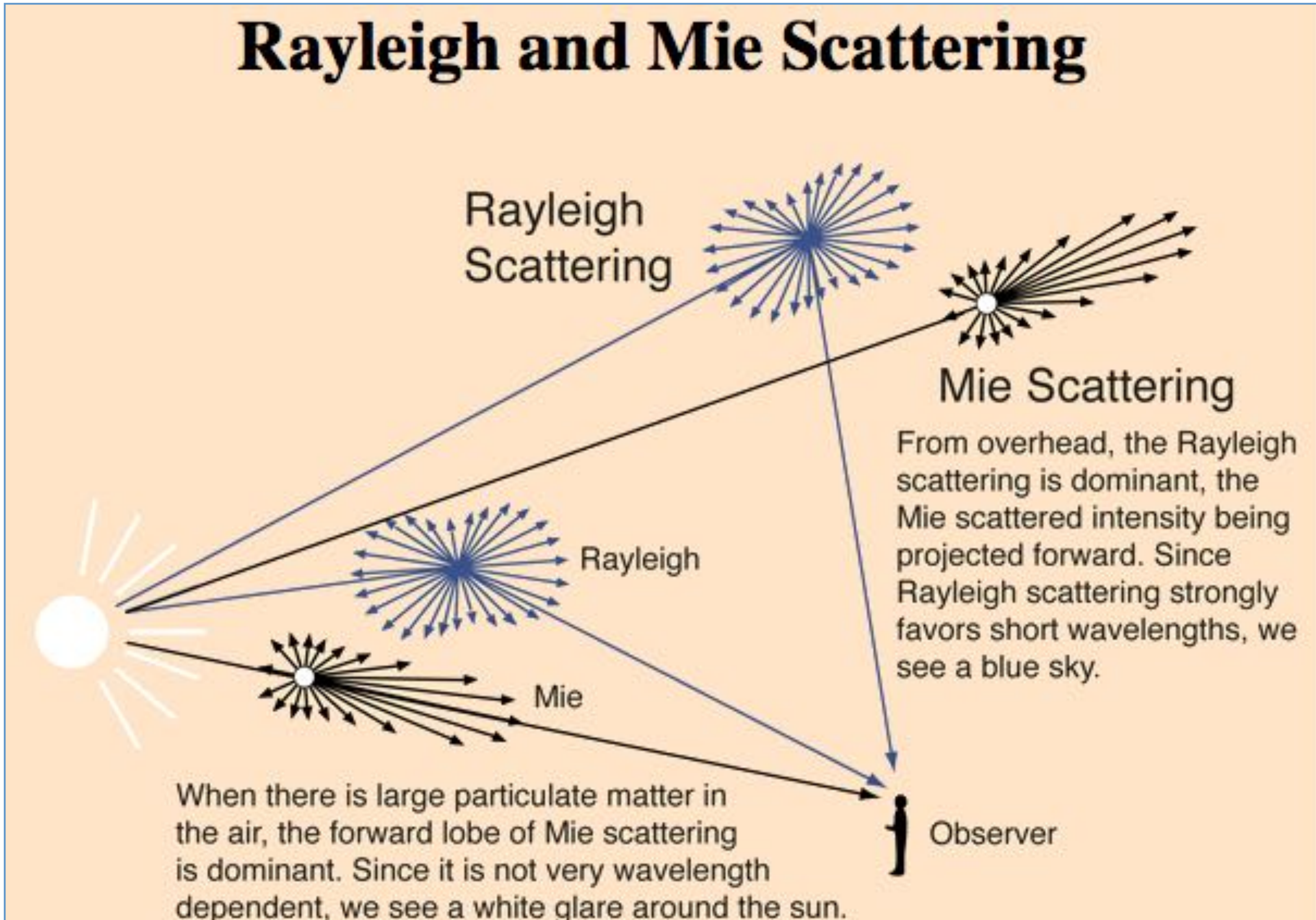
Rayleigh and Mie Scattering
Rayleigh Scattering
Mie Scattering
From overhead, the Rayleigh scattering is dominant, the Mie scattered intensity being projected forward. Since Rayleigh scattering strongly favors short wavelengths, we see a blue sky.
Rayleigh
Mie
When there is large particulate matter in the air, the forward lobe of Mie scattering is dominant. Since it is not very wavelength dependent, we see a white glare around the sun.
Observer

Halos

Sun Dogs

The 22° Halo

The familiar 22° halo around the Sun or Moon occurs because of refraction in tiny hexagonal ice crystals in the air. With the 60° apex angle of the prism formed by extending the sides of the crystal and the index of refraction of ice (n=1.31) one can calculate the angle of minium deviation to be 21.84°.

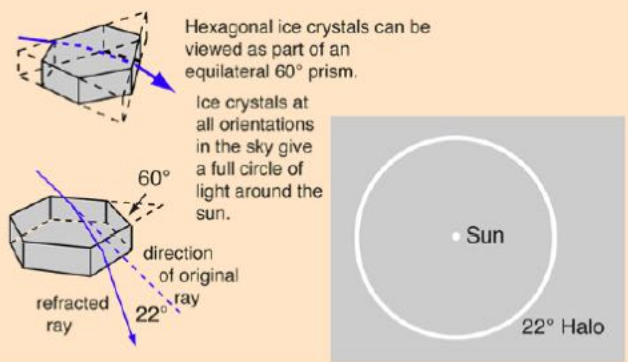

Sun Dogs (Parhelia)

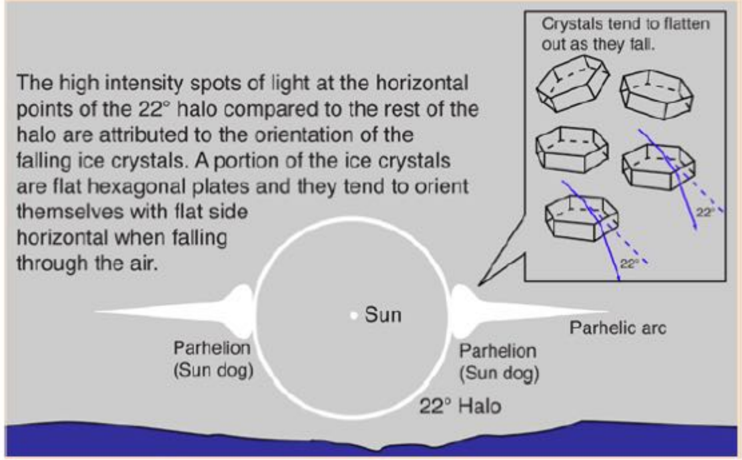

Eduardo Landul

MIE SCATTERING – TOWARDS A BIGGER SCATTERER

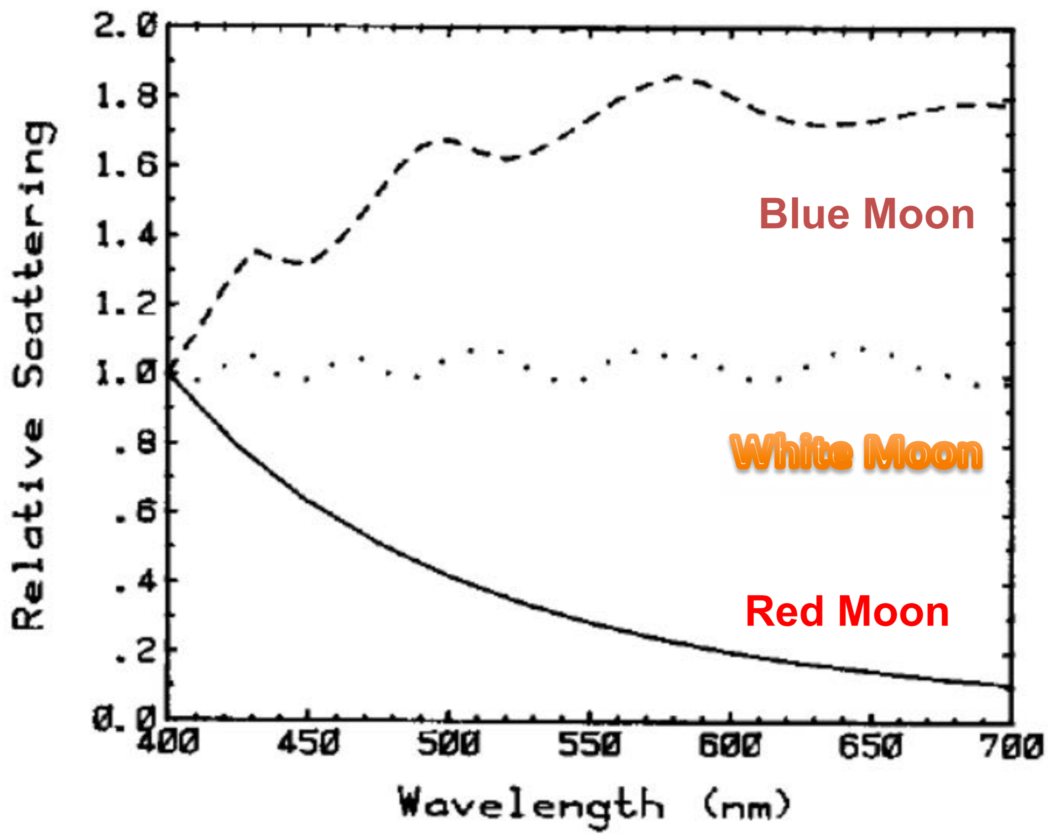

Fig. 8 Scattering of visible light by oil droplets of diameter 0.1 μm (solid curve), 0.8 μm (dashes), and 10 μm (dots)

Craig Bohren

MIE SCATTERING – AROUND A BIGGER SCATTERER

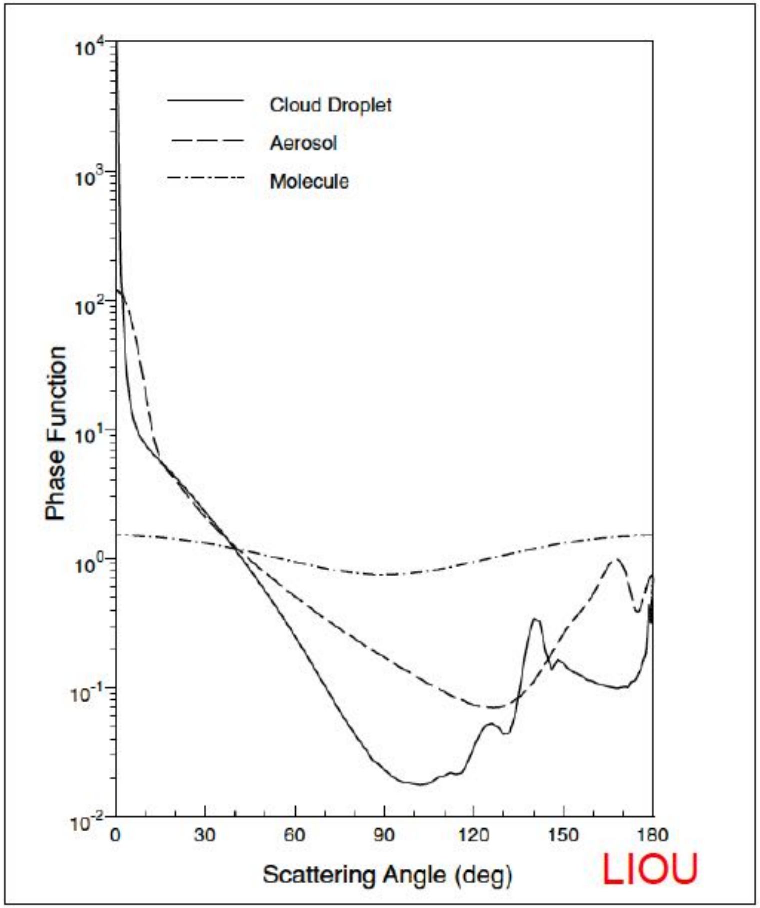

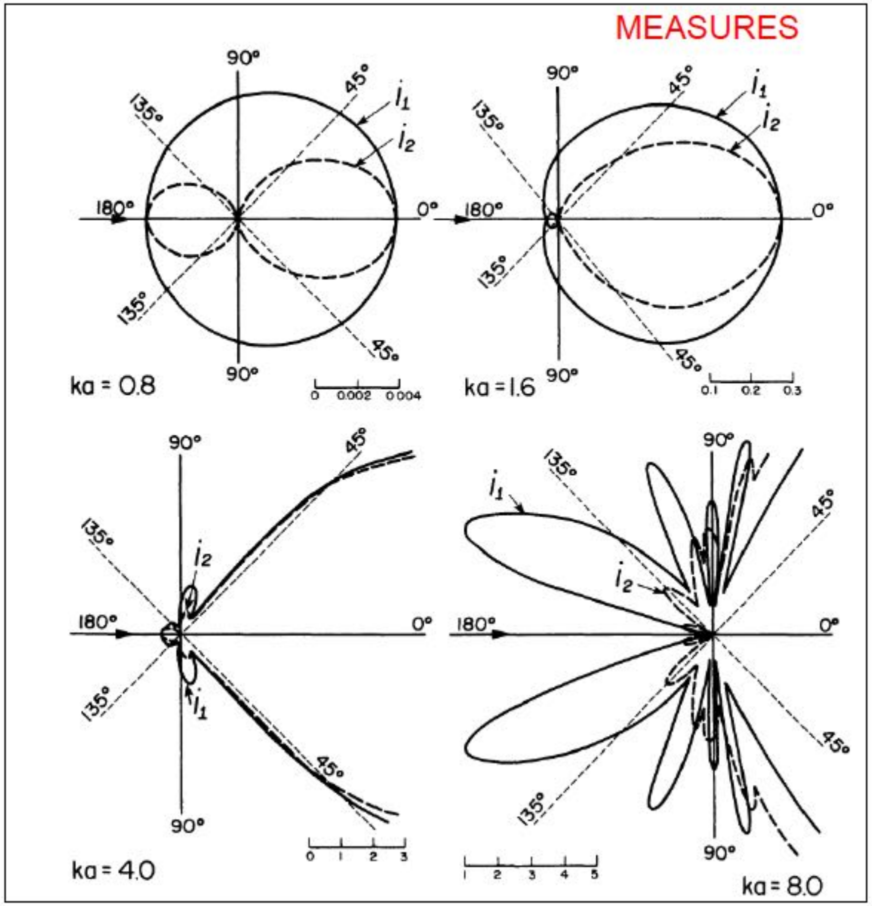

ka=x

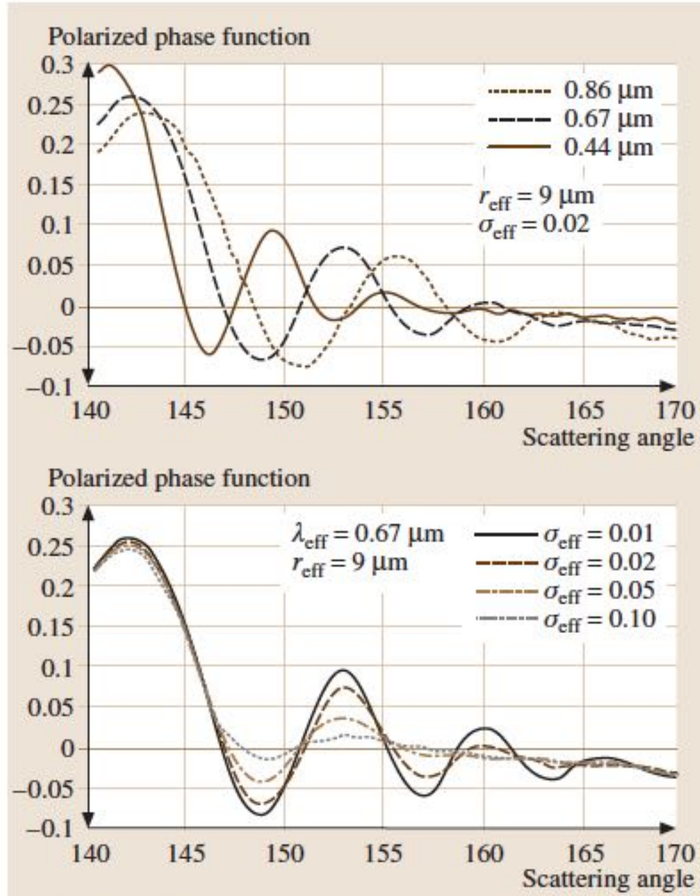

Fig. 19.2 Polarized Mie scattering phase function as a function of scattering angle for cloud droplet having a lognormal particle size distribution with an effective radius $r_{eff} = 9\,\mu m$. *Upper panel*: phase function as a function of wavelength with fixed $\sigma_{eff} = 0.02$ effective size variance; *lower panel*: as a function of effective size variance (courtesy of *Bréon* and *Goloub*, 2003)

MIE SCATTERING – SOME RESULTS

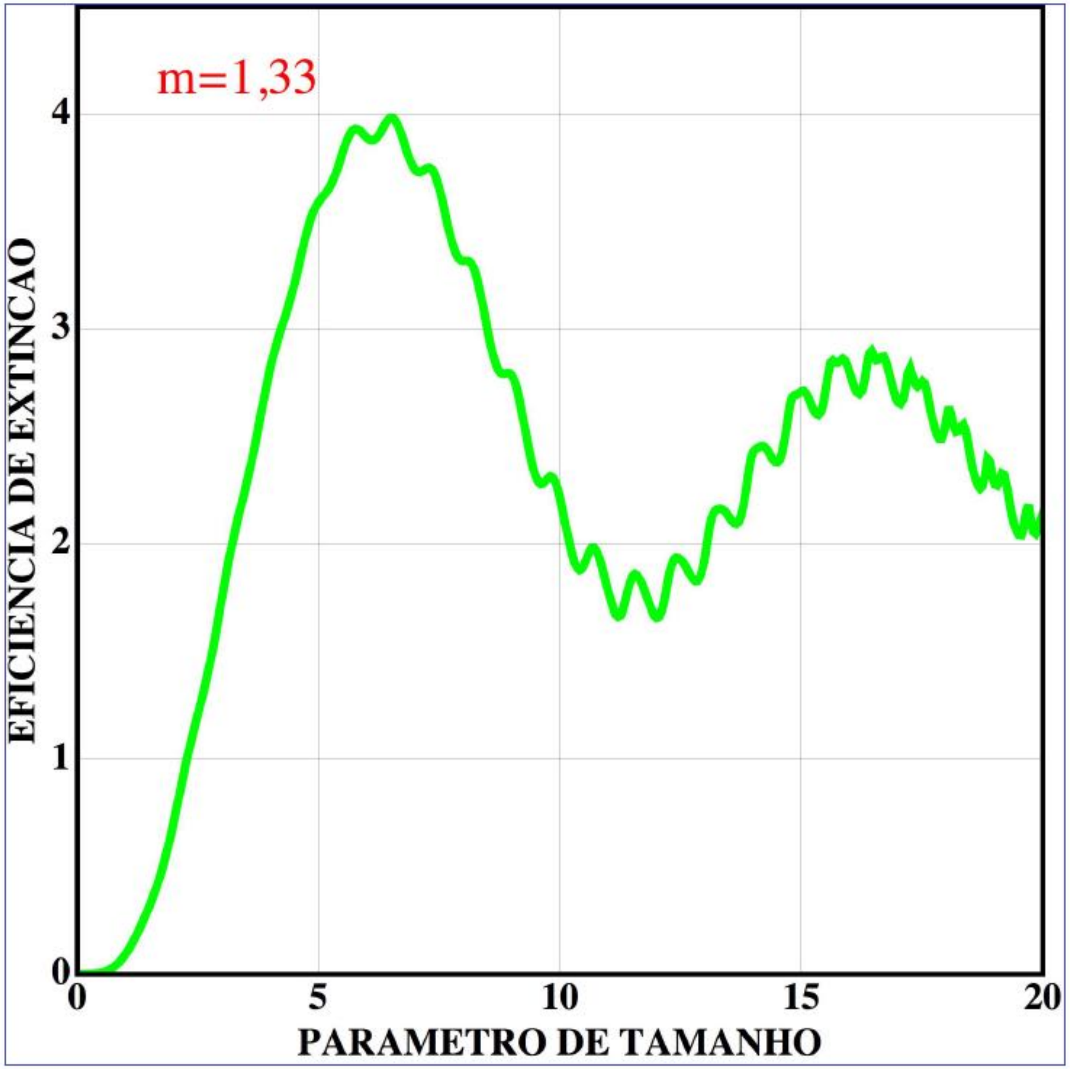

The image cannot be displayed. Your computer may not have enough memory to open the image, or the image may have been corrupted. Restart your computer, and then open the file again. If the red x still appears, you may have to delete the image and then insert it again.

MIE SCATTERING – SOME RESULTS

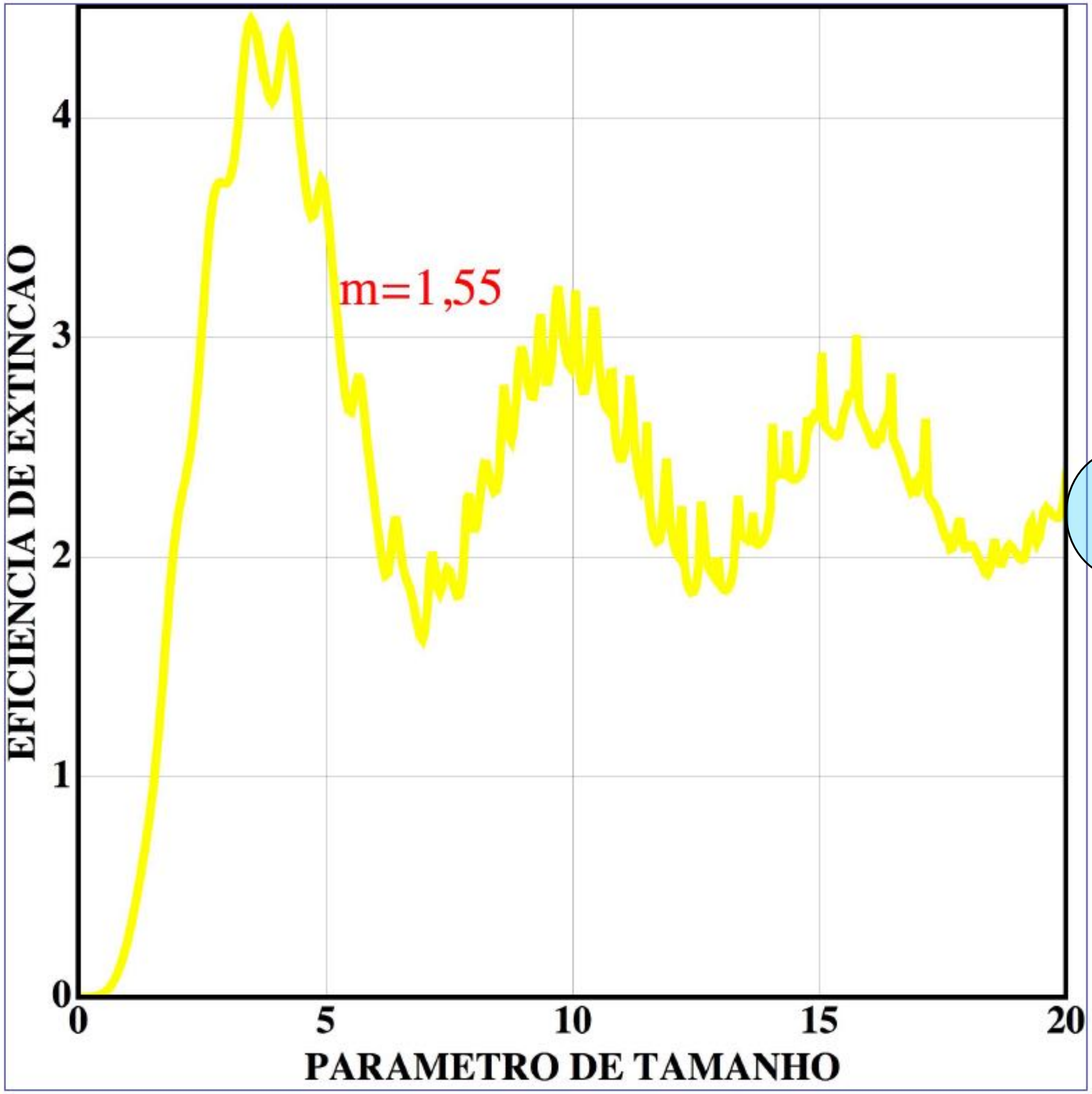

2

MIE SCATTERING - BUILDING CONCEPTS

WHAT'S THE TYPE OF SCATTERING ???

Passive remote sensing	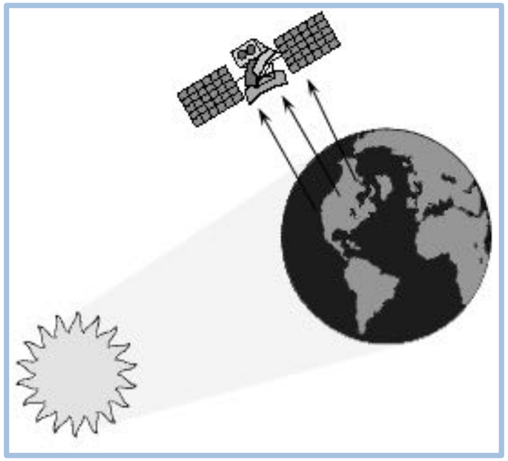	Based on"uncontroled illumination": - Sun - terrestrial emission	Passive methods: - extinction - scattering - longwave emission
Active remote sensing	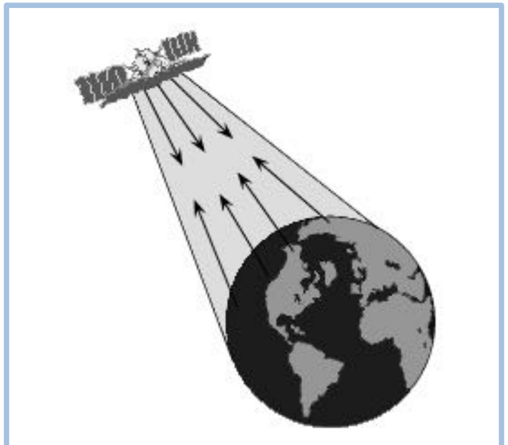	Based on "controled illumination" and measurement of backscattering	Active methods: - lidar - radar

Lidar (light detection and ranging) is an active remote sensing technology that measures distance by illuminating a target with a laser and analyzing the reflected light

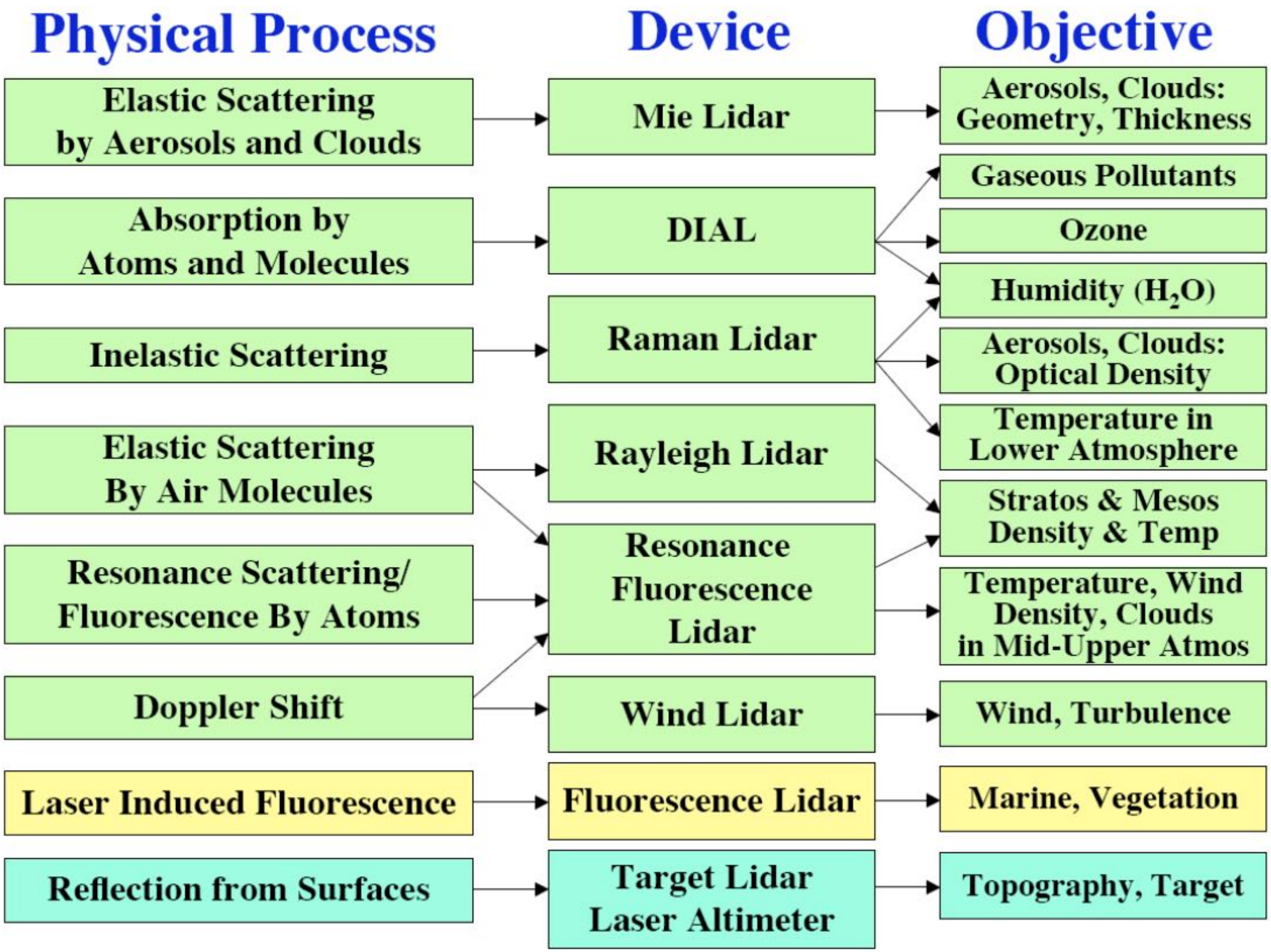
Physical Process
Device
Objective
Elastic Scattering by Aerosols and Clouds
Mie Lidar
Aerosols, Clouds: Geometry, Thickness
Absorption by Atoms and Molecules
DIAL
Gaseous Pollutants
Ozone
Humidity (H_2O)
Inelastic Scattering
Raman Lidar
Aerosols, Clouds: Optical Density
Temperature in Lower Atmosphere
Elastic Scattering By Air Molecules
Rayleigh Lidar
Stratos & Mesos Density & Temp
Resonance Scattering/ Fluorescence By Atoms
Resonance Fluorescence Lidar
Temperature, Wind Density, Clouds in Mid-Upper Atmos
Doppler Shift
Wind Lidar
Wind, Turbulence
Laser Induced Fluorescence
Fluorescence Lidar
Marine, Vegetation
Reflection from Surfaces
Target Lidar Laser Altimeter
Topography, Target

Laser-atmosphere interactions…

Laser – Atmosphere Interaction	Atmospheric Parameter-Species
Elastic Scattering ($\lambda_1=\lambda_2$)	Aerosols (PMs), clouds, atmospheric density, atmospheric structure, temperature…
Inelastic Scattering (Raman Scattering) ($\lambda_1=\lambda_2+\Delta\lambda_R$)	Water vapor, RH, O_3, temperature, Aerosols (extinction, backscatter coefficients)
Differential Absorption DIAL (λ_1, λ_2)	SO_2, O_3, NO_2, NO, CO_2, Hg, HF, HCl, NH_3, HCs, CO, H_2O
Resonance Scattering	K, Na, Li, Ca, Fe
Doppler shift	Wind measurements
Laser Induced Fluorescence (LIF)	OH^-

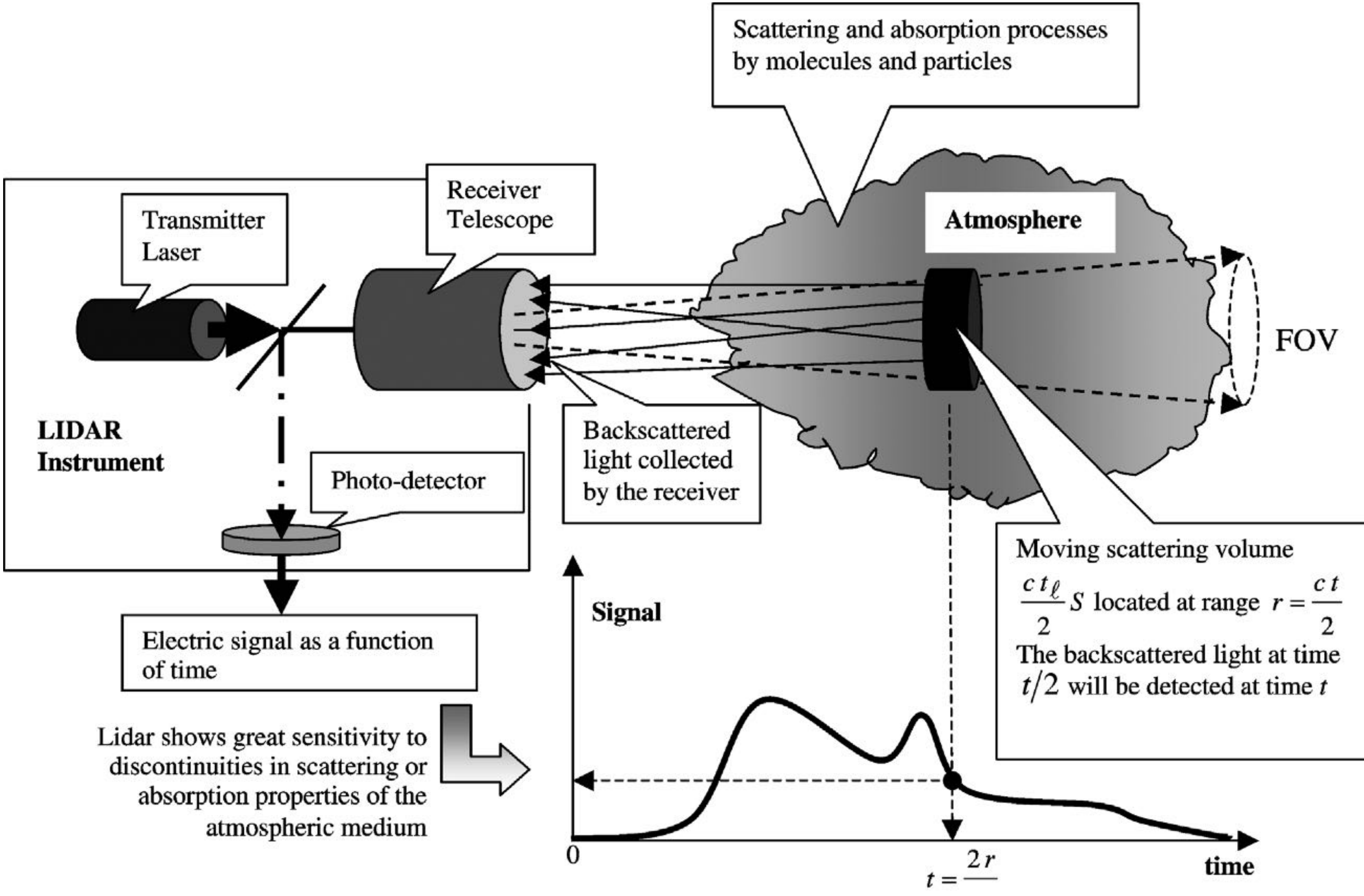
Scattering and absorption processes by molecules and particles
Receiver Telescope
Transmitter Laser
Atmosphere
FOV
LIDAR Instrument
Photo-detector
Backscattered light collected by the receiver
Moving scattering volume
$\frac{c\,t_\ell}{2} S$ located at range $r = \frac{c\,t}{2}$
The backscattered light at time $t/2$ will be detected at time t
Electric signal as a function of time
Signal
Lidar shows great sensitivity to discontinuities in scattering or absorption properties of the atmospheric medium
0
time
$t = \frac{2r}{c}$

REMOTE SENSING

LIDAR EQUATION- BUILDING CONCEPTS

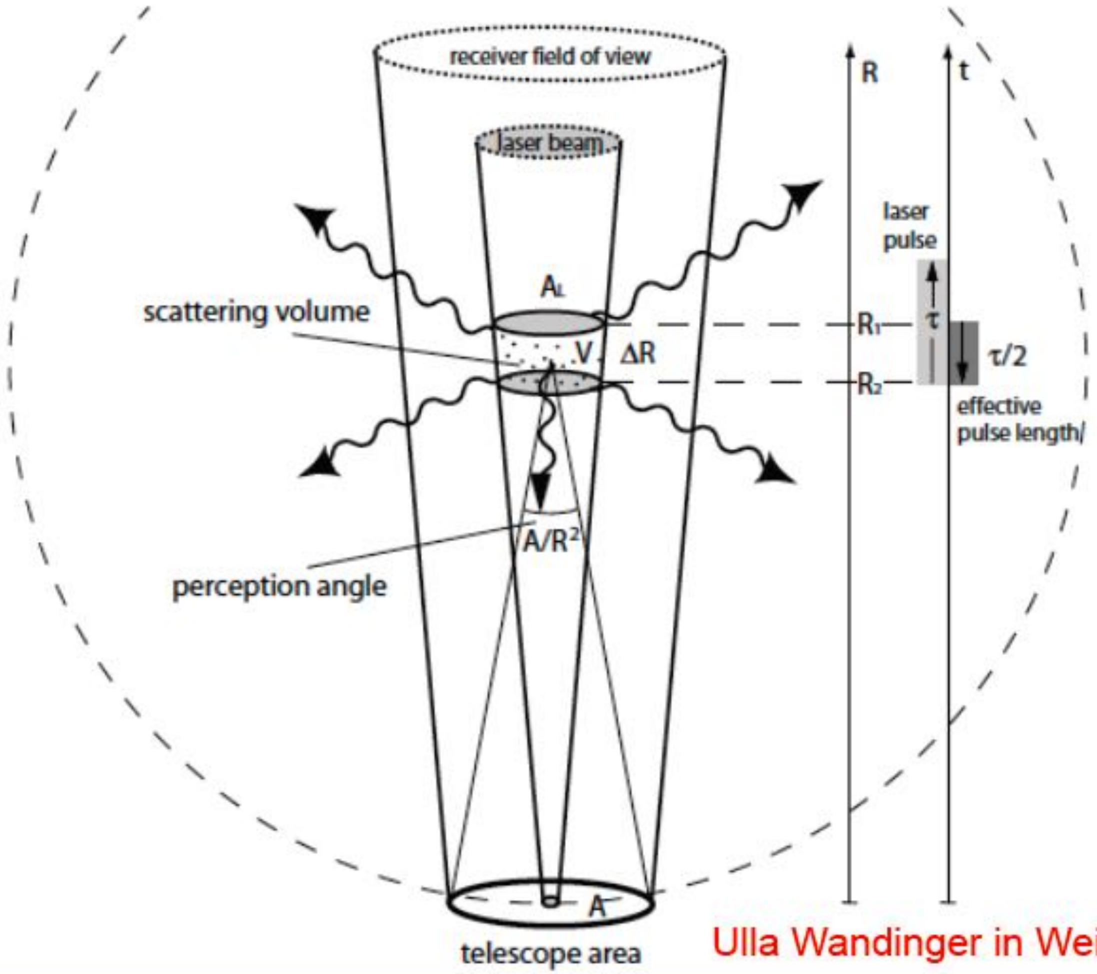

Ulla Wandinger in Weitkamp

LIDAR EQUATION – PROBED VOLUME

$$V_P = A_L . \Delta R$$

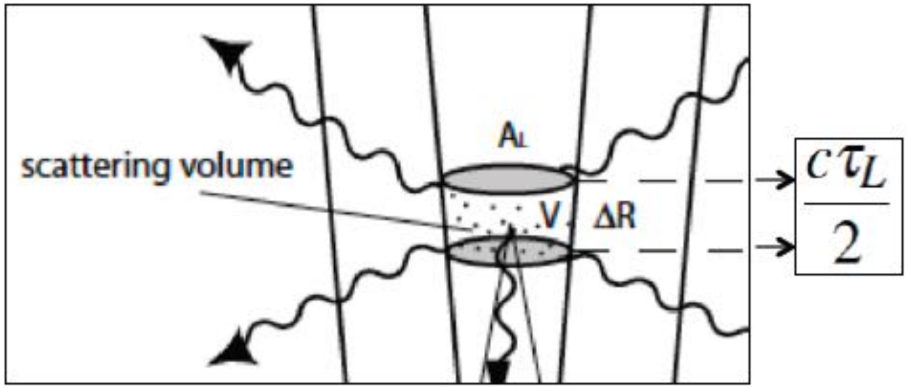

$$V_P = A_L . \frac{c\tau_L}{2}$$

LIDAR EQUATION- BUILDING CONCEPTS

At a given Range (R) and Wavelength (λ) :

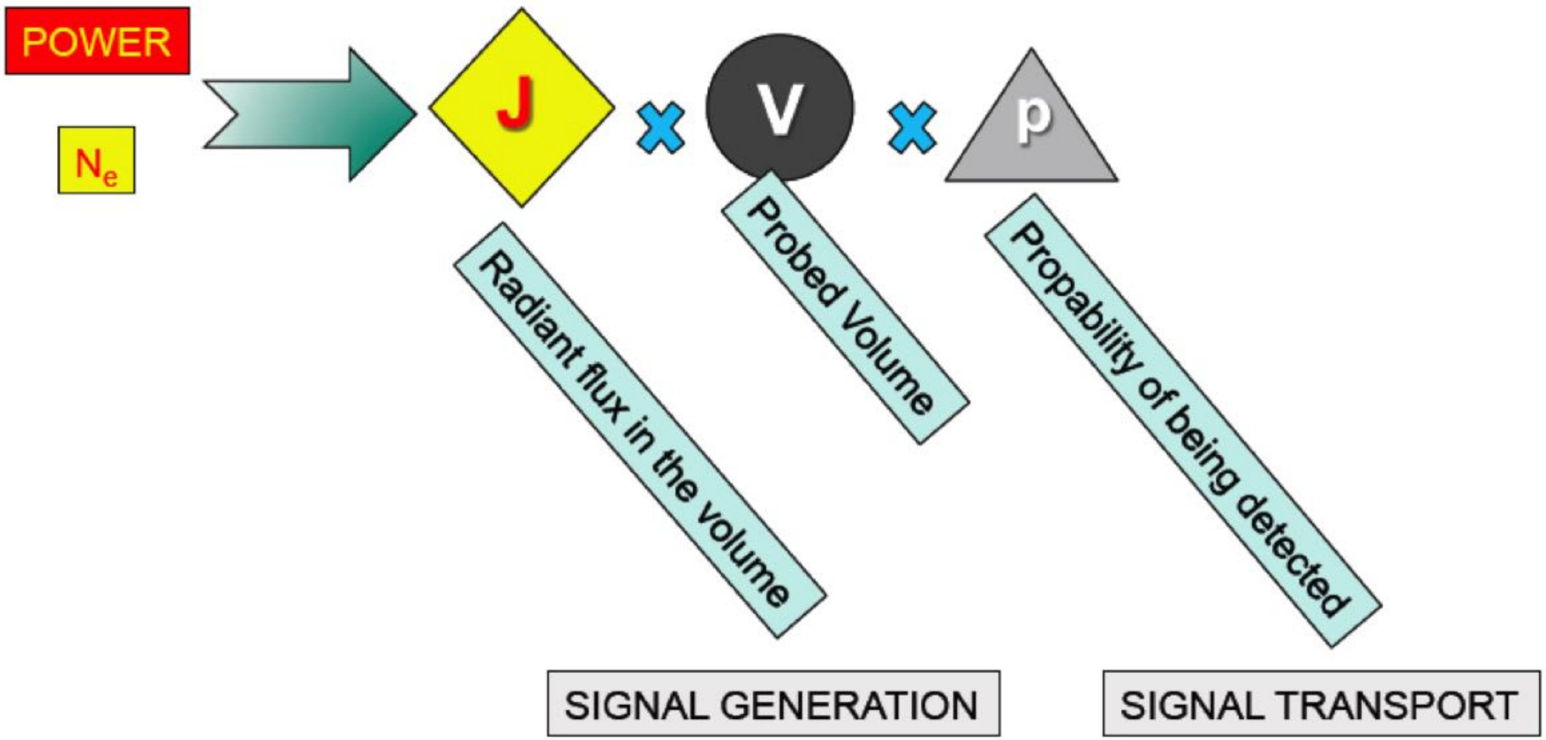

LIDAR EQUATION- BUILDING CONCEPTS

REMOTE SENSING

At a given Range (R) and Wavelength (λ) :

SIGNAL GENERATION

SIGNAL TRANSPORT

NATURE OF INTERACTION

INSTRUMENT + ATMOSPHERE

$$J(\lambda,R,r) = \beta_{\pi}(\lambda,R,r)I(R,r)$$

BACKSCATTERING

IRRADIANCE AT TARGET

$$p(\lambda,R,r) = \frac{A_o}{R^2} \times T(\lambda,R) \times \varepsilon(\lambda) \times \zeta(R,r)$$

ACCEPTANCE SOLID ANGLE

ATMOSPHERIC TRANSMISSION

SPECTRAL EFFICIENCY

GEOMETRIC FACTOR

LIDAR EQUATION- TRANSMISSION IN THE ATMOSPHERE

$$T(\lambda,r) \equiv e^{-2\int_0^R \alpha(\lambda,r)dr}$$

EXTINCTION COEFFICIENT

LIDAR EQUATION – THE FINAL CUT

$$J(\lambda, R, r) = \beta_\pi(\lambda, R, r) I(R, r)$$

✖

$$V_P = A_L . \frac{c\tau_L}{2}$$

✖

$$p(\lambda, R, r) = \frac{A_o}{R^2} \times T(\lambda, R) \times \varepsilon(\lambda) \times \zeta(R, r)$$

$$P_o = I(R, r).A_L$$

$$T(\lambda, r) \equiv e^{-2\int_0^R \alpha(\lambda, r) dr}$$

$$P(\lambda, R) = P_o \frac{A_o}{R^2} \beta_\pi(\lambda, R) \varepsilon(\lambda) \zeta(R) . \left(\frac{c\tau_L}{2}\right) e^{-2\int_0^R \alpha(\lambda, r) dR}$$

ELASTIC LIDAR EQUATION

LIDAR EQUATION – OVERLAP FUNCTION

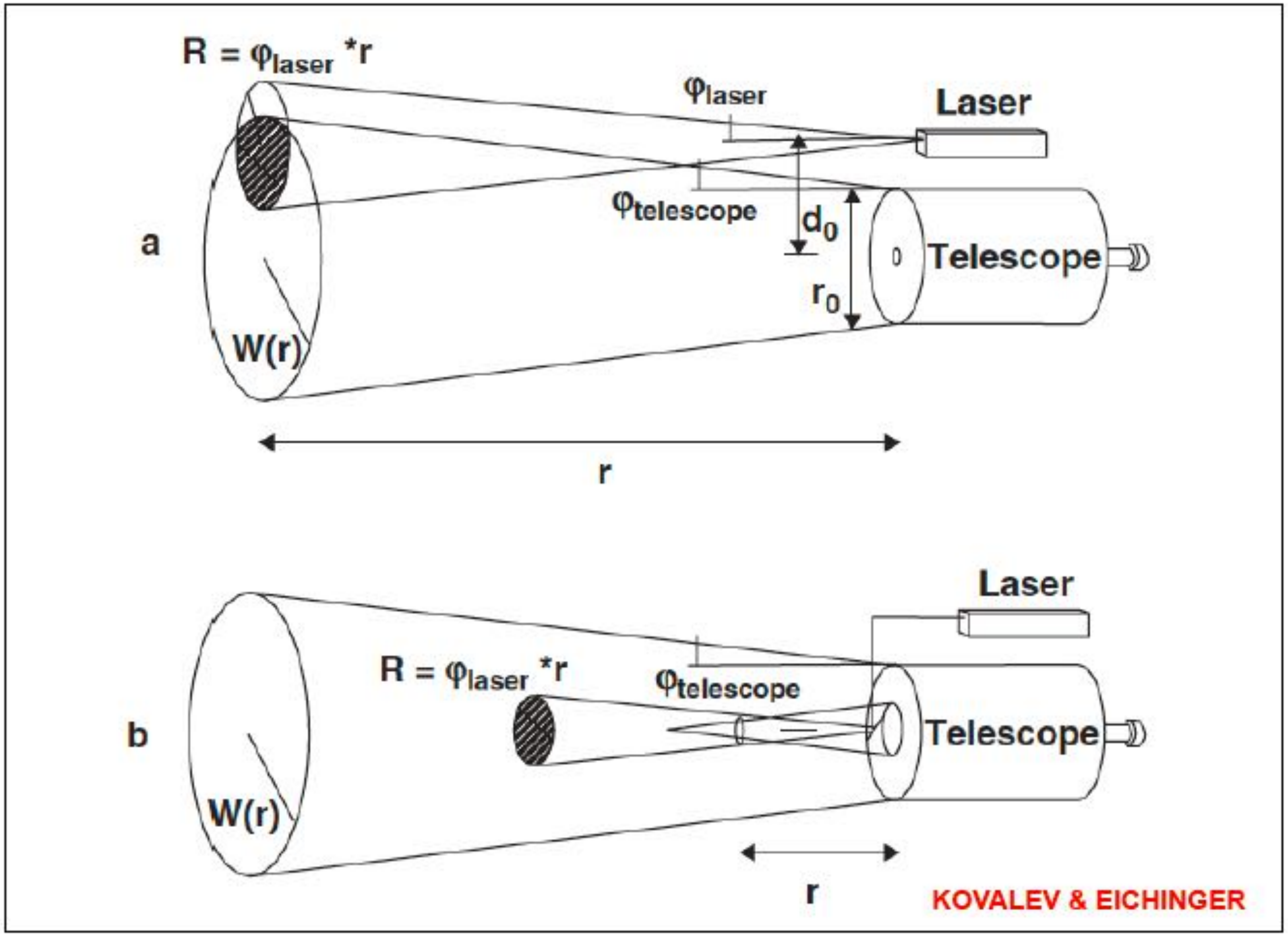

LIDAR EQUATION – OVERLAP FUNCTION

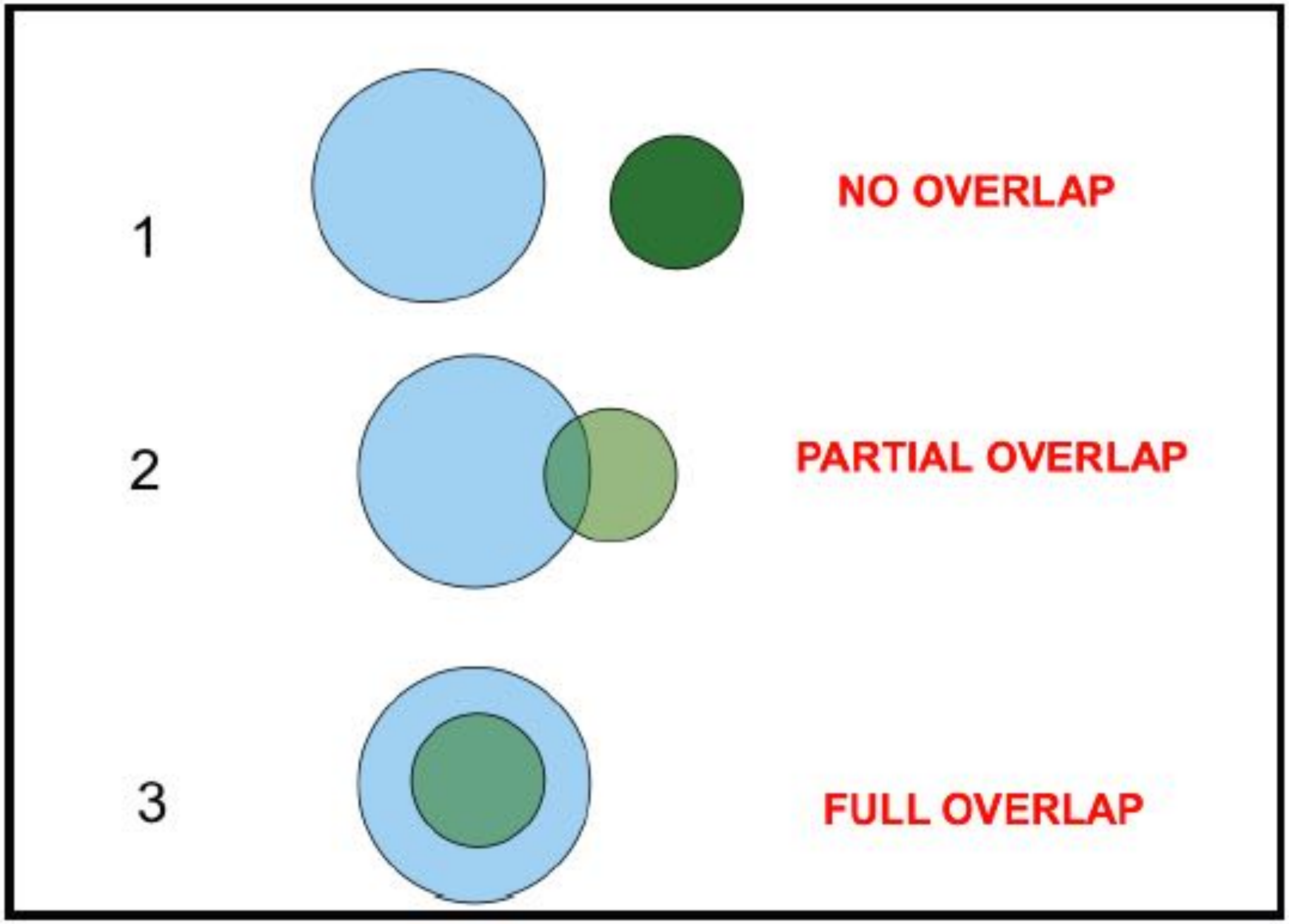

LIDAR EQUATION – SOLUTIONS

ATMOSPHERIC OPTICAL PARAMETERS

$$P(\lambda,R) = P_o \frac{A_o}{R^2} \beta_\pi(\lambda,R)\varepsilon(\lambda)\zeta(R).\left(\frac{c\tau_L}{2}\right) e^{-2\int_0^R \alpha(\lambda,r)dR}$$

BACKSCATTERING COEFFICIENT

$$[\beta(R)] = km^{-1}.sr^{-1}$$

EXTINCTION COEFFICIENT

$$[\alpha(R)] = km^{-1}$$

AEROSOL STUDIES WITH LIDARS – SOLUTIONS

LIDAR RATIO

$$P(\lambda,R) = P_o \frac{A_o}{R^2} \beta_\pi(\lambda,R) \varepsilon(\lambda) \zeta(R). \left(\frac{c\tau_L}{2}\right) e^{-2\int_0^R \alpha(\lambda,r) dR}$$

$$L_{aer}(R) = \frac{\alpha_{mol}(R)}{\beta_{mol}(R)} = \frac{8\pi}{3} sr$$

LIDAR RATIO (MOLECULAR)

$$L_{aer}(R) = \frac{\alpha_{aer}(R)}{\beta_{aer}(R)}$$

LIDAR RATIO (AEROSOL)

Vibration Raman lidar

- The technique:

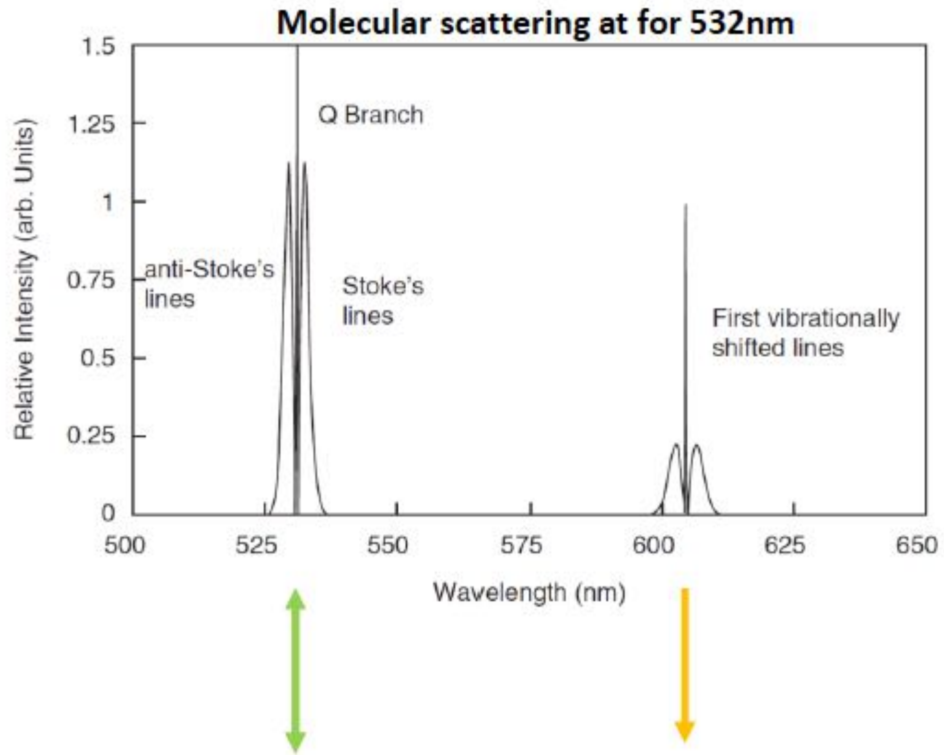

Emit
Detect (1)

Detect (2)

Image from Kovalev V.A. (2004)

Rotational Raman lidar

- The technique:

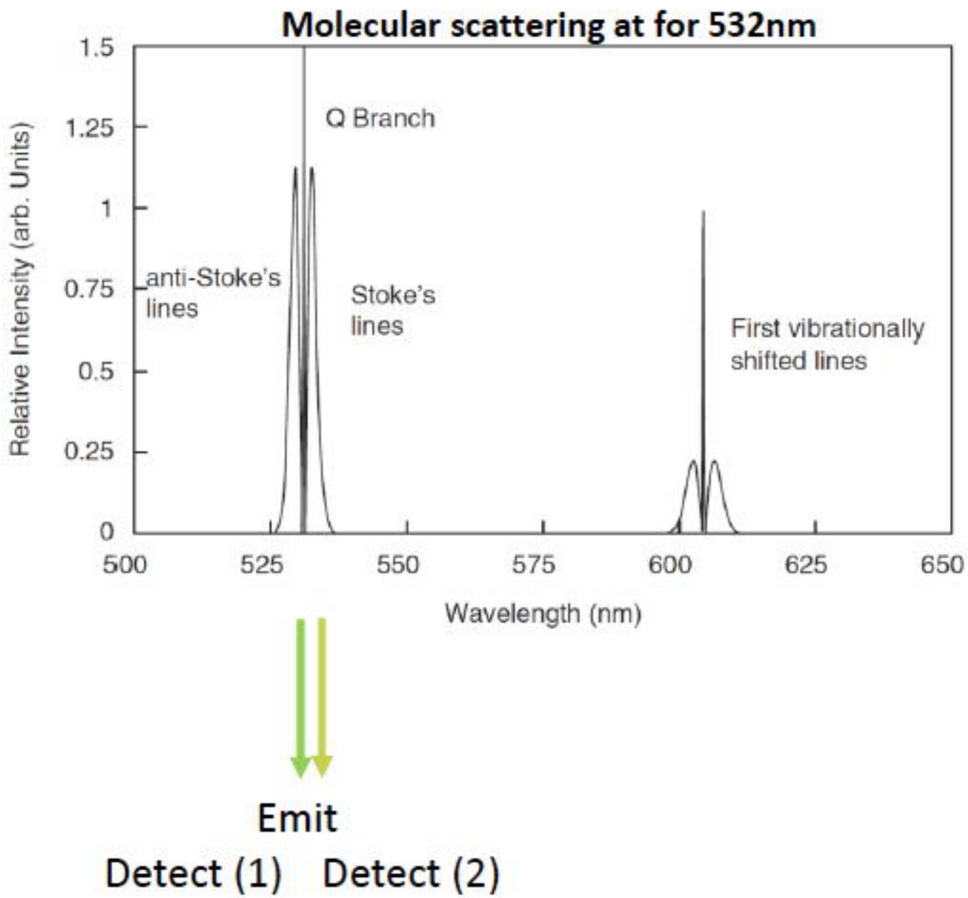

AEROSOL STUDIES WITH LIDARS – RAMAN LIDARS

$$P(\lambda,R) = P_o \frac{A_o}{R^2} \beta_\pi(\lambda_L, \lambda_R, R) \varepsilon(\lambda) \zeta(R). \left(\frac{c\tau_L}{2}\right) e^{-\int_0^R \alpha(\lambda_L, r) + \alpha(\lambda_R, r) dR}$$

↓

RAMAN SCATTERING CROSS SECTION

↓

DIFFERENTIAL TRANSMISSION

AEROSOL STUDIES WITH LIDARS – RAMAN LIDARS

$$\alpha(355, z) = \frac{\frac{d}{dz}\left[ln\frac{N(z)}{z^2 P(z)}\right] - \alpha_{mol}(355, z) - \alpha_{mol}(387, z)}{1 + \frac{355}{387}}$$

$\lambda_L = 355$ nm

$\lambda_R = 387$ nm

NITROGEN RAMAN SCATTERING

$\lambda_L = 355$ nm

AEROSOL STUDIES WITH LIDARS – HRSL LIDARS

HIGH RESOLUTION SPECTRAL LIDARS

AEROSOL DOPPLER BROADENING

MOLECULAR DOPPLER BROADENING

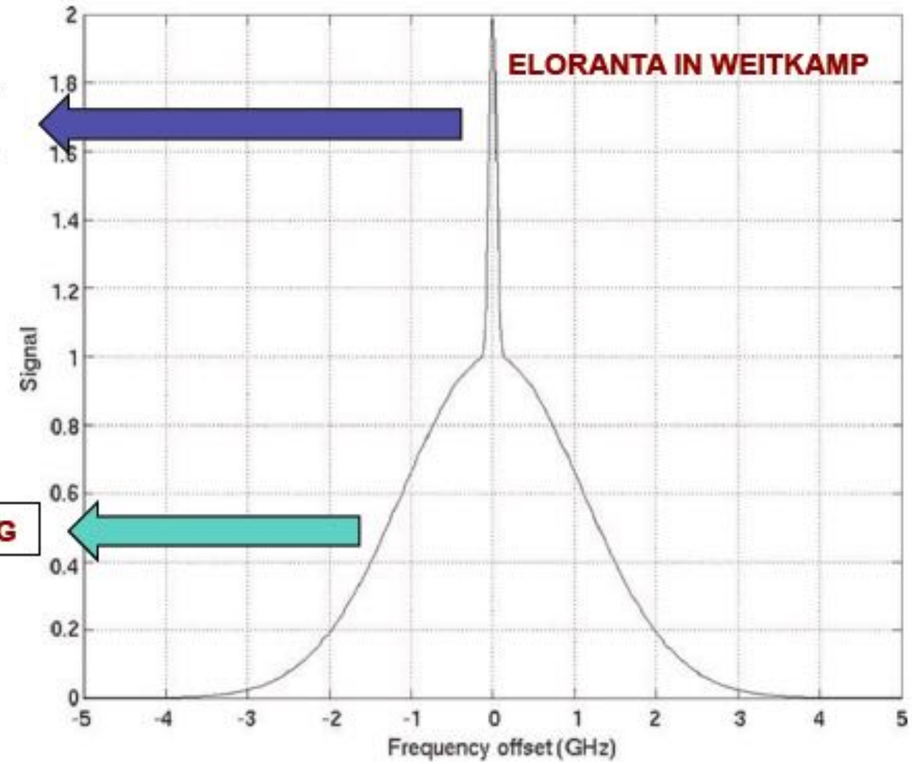

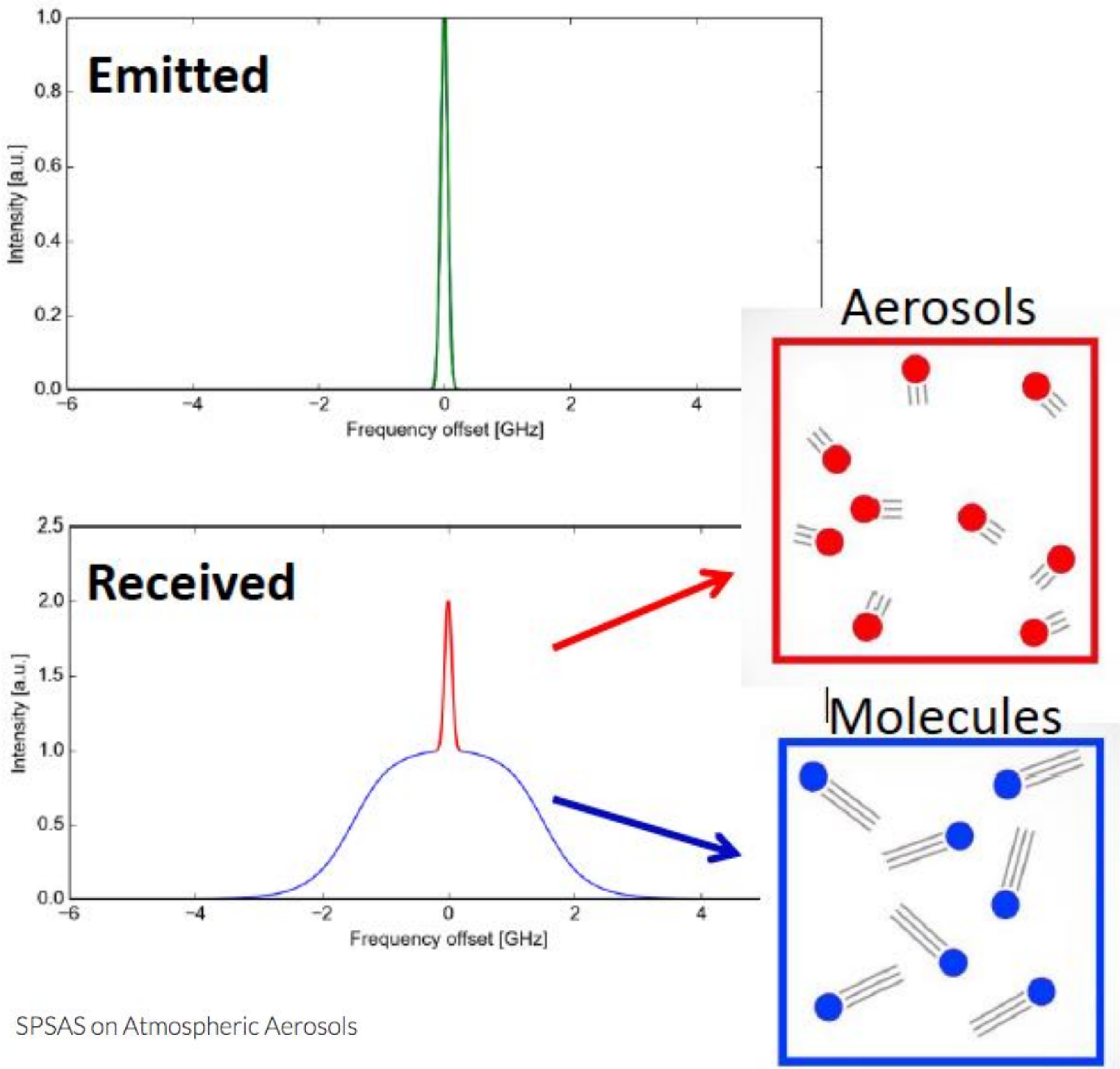
Emitted
Intensity [a.u.]
1.0
0.8
0.6
0.4
0.2
0.0
−6
−4
−2
0
2
4
Frequency offset [GHz]
Received
2.5
2.0
1.5
1.0
0.5
0.0
Aerosols
Molecules

AEROSOL STUDIES WITH LIDARS – HRSL LIDARS

HIGH RESOLUTION SPECTRAL LIDARS

$$P_{\mathrm{mol}}(r) = K_{\mathrm{mol}} r^{-2} O(r) \beta_{\mathrm{mol}}(r) \exp\left(-2\int_0^r \alpha(r')\mathrm{d}r'\right)$$

$$P_{\mathrm{aer}}(r) = K_{\mathrm{aer}} r^{-2} O(r) \beta_{\mathrm{aer}}(r) \exp\left(-2\int_0^r \alpha(r')\mathrm{d}r'\right)$$

$$\Re(r) = \frac{\beta_{\mathrm{aer}}(r)}{\beta_{\mathrm{mol}}(r)} = \frac{K\, P_{\mathrm{aer}}(r)}{P_{\mathrm{mol}}(r)}.$$

Teramobile LIDAR

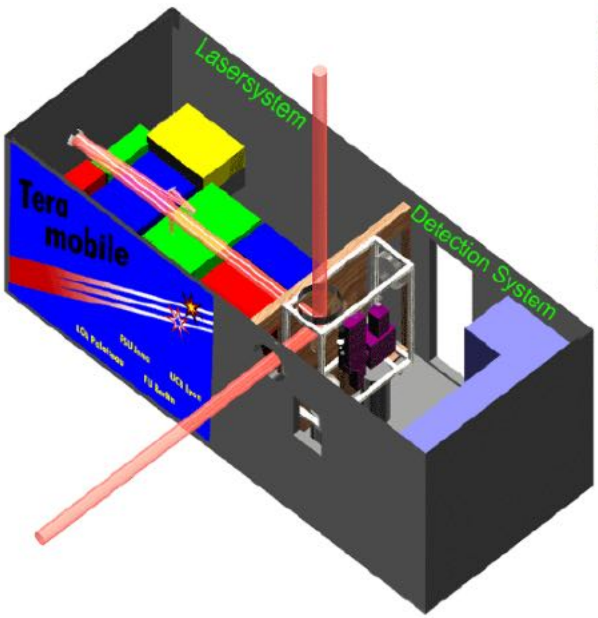

Kasparian J. et al, Science, 301, 61, 2003]

The TERAMOBILE laser

Laser Parameters :
790 nm
350 mJ
60 fs
5 TW

Teramobile LIDAR

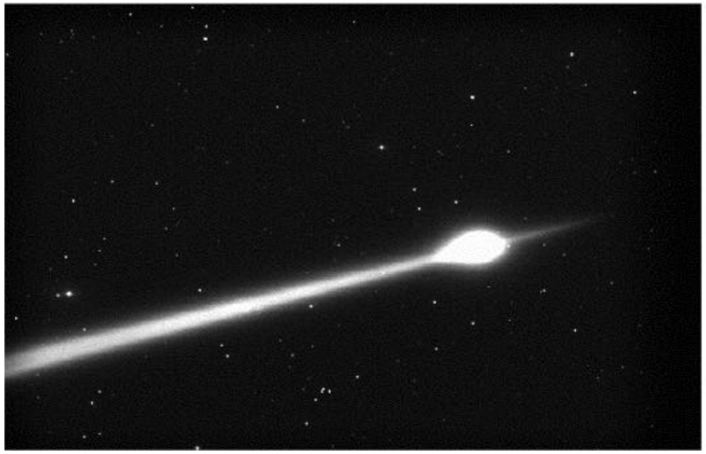

Femtosecond lidar

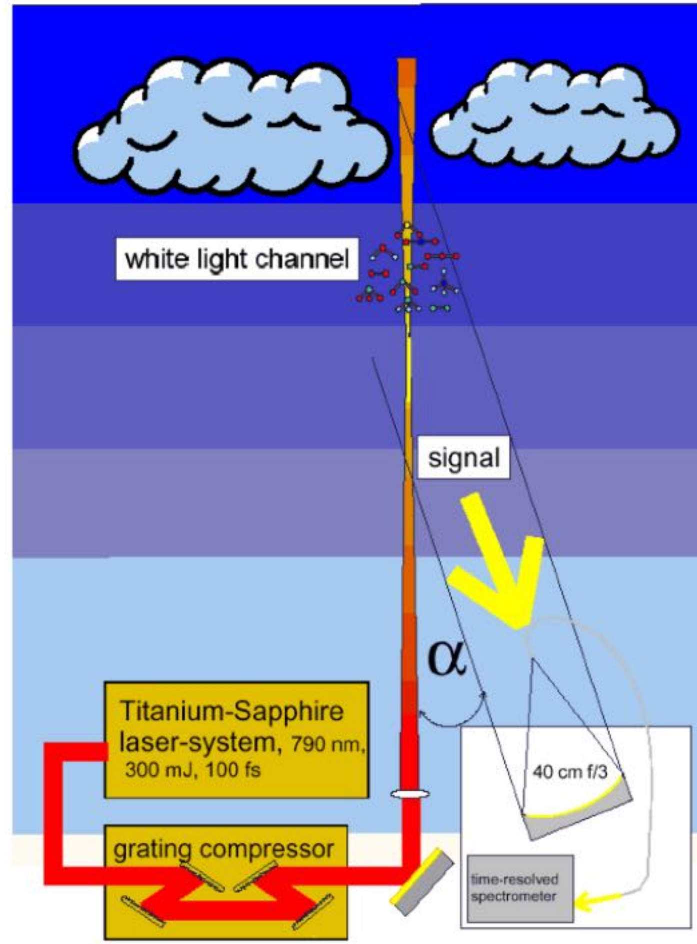

[Kasparian J. et al, Science, 301, 61, 2003]